MULTISCALE MODEL. SIMUL.
Vol. 12, No. 1, pp. 364–395

CONNECTION OF KINETIC MONTE CARLO MODEL FOR SURFACES TO ONE-STEP FLOW THEORY IN 1+1 DIMENSIONS*

PAUL N. PATRONE† AND DIONISIOS MARGETIS‡

Abstract. The Burton–Cabrera–Frank (BCF) theory of step flow has been recognized as a valuable tool for describing nanoscale evolution of crystal surfaces. We formally derive a single-step BCF-type model from an atomistic, kinetic Monte Carlo (KMC) model of a crystal surface in 1+1 dimensions without external material deposition. Through an averaging procedure, consistent with Boltzmann statistics, we introduce definitions of the continuous quantities of the BCF theory, i.e., the step position and density of adsorbed atoms (adatoms), as expectation values taken over the discrete probabilities of the KMC model. The equations of our BCF-type model describe the time evolution of these expectation values. A central idea of our approach is to exploit the observation that the number of adatoms on a surface is typically small at experimentally relevant temperatures. Accordingly, we (i) show that our BCF-type theory arises from a KMC model in which only one adatom is allowed to move, and (ii) characterize corrections to the theory, which come from correlations between two or more atoms. We derive (via a discrete maximum principle) a criterion on the initial conditions under which such corrections are negligible for all times; this allows us to interpret our BCF-type model as a near-equilibrium theory. Our approach reveals the atomistic origins of the material parameters entering the BCF model.

Key words. kinetic Monte Carlo, Burton–Cabrera–Frank theory, low-density approximation, near-equilibrium condition, master equation, maximum principle

AMS subject classifications. 74A50, 35R35, 82C05, 82C80

DOI. 10.1137/13091587X

1. Introduction.

In the many years since it was first proposed, the Burton–Cabrera–Frank (BCF) model [5] of step flow has been recognized as a useful tool for describing near-equilibrium crystal surface evolution. The BCF theory has been invoked in studies that span a range of topics, including electromigration of atoms and step bunching [28, 43, 44, 45], surface relaxation [16, 17], stochastic fluctuations of surface defects [11, 25, 27, 28, 31, 32, 33, 34], and faceting [17, 45], to name a few. Moreover, the theory has served as a starting point from which fully continuum models, such as partial differential equations for the surface height, are derived; see, e.g., [8, 21, 28, 46].

Mathematically, the BCF model is a description of surface evolution in terms of a

*Received by the editors April 5, 2013; accepted for publication (in revised form) December 5, 2013; published electronically March 20, 2014. This research was supported by NSF DMS0847587 at the University of Maryland. This work was performed by an employee of the U.S. Government or under U.S. Government contract. The U.S. Government retains a nonexclusive, royalty-free license to publish or reproduce the published form of this contribution, or allow others to do so, for U.S. Government purposes. Copyright is owned by SIAM to the extent not limited by these rights.

http://www.siam.org/journals/mms/12-1/91587.html

†Center for Nanoscale Science and Technology, National Institute of Standards and Technology, Gaithersburg, MD 20899-1070, and Department of Physics, Institute for Research in Electronics and Applied Physics, and Condensed Matter Theory Center, University of Maryland, College Park, MD 20742-4111 (ppatrone@umd.edu). This author's research was supported by the National Institute of Standards and Technology American Recovery and Reinvestment Act Measurement Science and Engineering Fellowship Program award 70NANB10H026 through the University of Maryland, with ancillary support from the NSF MRSEC under grant DMR 05-20471 and the Condensed Matter Theory Center.

‡Department of Mathematics, and Institute for Physical Science and Technology, and Center for Scientific Computation and Mathematical Modeling, University of Maryland, College Park, MD 20742-4015 (dio@math.umd.edu).

Stefan-type problem [12, 37]. The theory accounts for the diffusion of adsorbed atoms (adatoms) on terraces between steps; the steps are free boundaries whose motion results from attachment or detachment of atoms. Despite the physical appeal of this picture, however, the connection of the BCF theory to a fully atomistic model of surface diffusion is not well understood. Consequently, many questions remain regarding the underlying assumptions and physical processes that give rise to the BCF theory. Moreover, in many applications of epitaxial growth, it is desirable to know, from an atomistic perspective, when the BCF model breaks down or how it can be extended beyond the near-equilibrium regime [30].

In this paper, our main goal is to formally derive a BCF-type model from an atomistic, kinetic Monte Carlo (KMC) description of the surface.[1] We limit our analysis to a single step in a one-dimensional (1D) setting without external material deposition. In the course of our derivation, we seek conditions ensuring that the BCF model remains consistent with the KMC theory for all times. Toward this end, we express the atomistic rules for surface evolution in terms of a master equation and carry out the following tasks:

(i) define the step position and adatom density as appropriate averages coming from the master equation;

(ii) show how the BCF model, *with correction terms accounting for adatom correlations*, describes the time evolution of these averages; and

(iii) by using a discrete maximum principle, show that the temperature and initial adatom density control the size of the corrections to the BCF model.

The central idea of our approach is to exploit the fact that, for many materials undergoing relaxation at low enough temperatures, the number of adatoms on a surface is typically small. This fact has been predicted by theory [14, 18] *and observed experimentally* [54]. Consequently, we expect that at sufficiently low temperatures, the motion of a few isolated adatoms (as opposed to the correlated motion of many adatoms) should be the dominant physical process driving surface evolution.

These observations motivate two key aspects of our approach. First, we study only a one-step system. Since many systems are found to be in a low-density regime irrespective of the number of steps on the surface, we believe that the addition of more (noninteracting) steps does not significantly alter the dominant evolution process, i.e., single-adatom motion.

Second, we decompose the KMC master equation, which accounts for the motion of m atoms (m-p model), into a Bogoliubov–Born–Green–Kirkwood–Yvon (BBGKY)-type hierarchy whose nth level describes the evolution of the n-adatom joint probabilities. Our analysis shows that the single-adatom probabilities play the dominant role in surface evolution, which leads us to truncate the hierarchy, yielding the one-particle (1-p) model. We show how the BCF model can be derived from this 1-p model and find that corrections come from the multi-adatom joint probabilities. The size of the corrections is controlled by the temperature, which we treat as a small parameter.[2] Here we use the term *low-density regime* to describe systems with only one adatom and refer to the neglect of the multi-adatom joint probabilities as the

[1] We use the phrase "BCF-type" since our models do not account for step curvature, which is considered in the original work [5]. We sometimes refer to our BCF-type model as a *step continuum* model [18].

[2] We always compare the temperature to the bond energy E_b between atoms in the lattice. Temperatures as high as 1000 K (not unusual for experiments) are often small relative to E_b.

low-density approximation.[3]

A critical task that we address is to reconcile the atomistic nature of the KMC model with the notions of a continuous adatom density and step position in the BCF theory. *In particular, this reconciliation must resolve the question of how a step can be defined in terms of the atomistic geometry.* We take the viewpoint that a KMC model recognizes only the bonding between and motion of individual atoms. At the atomistic scale, we define the step position as the location of the atom (i) with one in-plane neighbor, and (ii) having the property that all atoms in its neighbor's direction have two in-plane nearest neighbors. We therefore define the step position and adatom density of our BCF-type theory as suitable expectation values taken over the allowed atomistic configurations, whose probabilities evolve according to the master equation. Here, our definition implies the existence of the step for all times and is consistent with Boltzmann statistics[4] when the system approaches equilibrium.[5]

Previous studies [1, 26, 38, 39, 53] of the connection between KMC descriptions and the BCF theory have focused on deriving or verifying individual parts of the latter (cf. section 1.2). Here, we are interested in deriving the entire BCF theory (i.e., the diffusion equation, kinetic relations, and step velocity law) in order to understand the connection between its elements. Moreover, our analysis (which is restricted to 1+1 dimensions) is meant to establish techniques that can be generalized to surfaces with richer effects, such as external material deposition, interacting steps, and (2+1)-dimensional geometries. Hence, this paper is the first in a series that aims to address increasingly complicated aspects of the BCF theory.

Despite its simplicity, however, our (1+1)-dimensional model provides significant insight into the physics of the BCF theory. By exposing the central role of the low-density approximation, our derivation (i) reveals how lowering the temperature decreases both the number of atoms that detach from the step and (consequently) the adatom correlations on the terrace, leading to a better agreement of our KMC scheme with the BCF theory; and (ii) indicates what terms, reflecting certain atomistic processes, must be added to the BCF equations to describe higher-density regimes. These observations can therefore (i) explain the widespread applicability of the BCF theory as coming from generic properties (e.g., having low adatom densities) of a large class of physical systems; and (ii) suggest modifications to extend the predictive power of the BCF theory.

1.1. Surfaces at two scales. This section provides a brief introduction to the KMC and BCF perspectives. Our exposition may be skipped in favor of sections 3–6. The interested reader may consult [4, 13, 52] for a review of generic KMC algorithms; see also [2, 6, 50] for examples of KMC simulations applied to crystal surfaces.

1.1.1. Kinetic Monte Carlo approach. In the context of surfaces, the KMC approach is a probabilistic representation of the system that accounts for the random motion (hopping) of individual atoms. Solutions to a KMC model are the time-

[3]The term "low-density regime" anticipates one of our main results, since we have not yet discussed any *densities* at this point. In sections 4, 5, and 6 we show, via a suitable averaging procedure, that one-adatom states correspond to a low number-density of adatoms on the surface (see also the following paragraph). The role of the 1-p model here bears some resemblance to the well-known notion of an ideal gas, which has been invoked in previous studies of the BCF theory [33].

[4]We use the term "Boltzmann statistics" to emphasize that the total number of atoms is fixed in our system, meaning that the appropriate description is based on the canonical ensemble. In contrast, the term "Gibbs distribution" would be appropriate for a perspective in which the number of atoms is not fixed.

[5]In our approach, whether or not steps form spontaneously depends on the definition of a step.

dependent, joint probabilities of finding the system in each atomistic configuration. The model itself describes how the system transitions between these configurations.

We consider a typical bond-counting, solid-on-solid model [18, 51]. The system evolves by means of hopping events in which a single atom is chosen at random to move to an adjacent lattice site. The probability with which an atom is picked is given in terms of a transition rate $k(n) \sim De^{-E_b n/k_B T}$, where D is the hopping rate for adatoms with no in-plane nearest neighbors, E_b is a bond energy, n is the number of in-plane nearest-neighbor bonds that the moving particle breaks, k_B is Boltzmann's constant, and T is the absolute temperature ($k_B T$ is the Boltzmann energy). The parameters E_b and D are material dependent (whereas the temperature T is adjustable). A set of transition rates and initial probabilities are sufficient to determine the probabilities of any configuration at any later time [6, 18, 48, 50]. Since we do not consider external material deposition, the transition rates are chosen such that (i) detailed balance is satisfied, and (ii) the total mass remains constant. See section 3.1 and Remark 4.3 for more details on the transition rates.

We use two different approaches, one numerical and one analytical, to model surfaces from a KMC perspective. In the numerical approach, computer simulations exploit random number generators in order to realize many elements of the statistical ensemble describing the system. Given enough elements from the ensemble, one can approximate the time-dependent, joint probabilities for each atomistic configuration [2, 50]; see section 3 for results of our KMC simulations.

In the analytical approach, we define a system of linear differential equations (called the "master equation" in this context) that describes the evolution of the probabilities for each atomistic configuration. We index these configurations with $i = 1, 2, \ldots$ and write the master equation in the form

$$\dot{p}_i(t) = \sum_j T_{i,j}(k) p_j(t), \tag{1.1}$$

where p_i is the probability of the ith configuration, $k \sim De^{-E_b n/k_B T}$ (defined above), and $\mathbf{T} = [T_{i,j}]$ (henceforth referred to as the T-matrix)[6] has the probability conserving property that $\sum_i T_{i,j} = 0$ for all j. See [7] for a current review of the master equation approach applied to nonequilibrium systems; see sections 5 and 6 for particular cases of (1.1).

1.1.2. BCF-type model. A BCF-type model describes the system evolution in terms of a free boundary problem [5]. The surface is divided into one or more nanoscale domains called terraces, which are separated by moving boundaries, steps. An adatom density, which obeys a diffusion equation, represents adatoms on the terraces. Solving the BCF model yields the adatom density and step positions as functions of time; see Figure 1(a), as well as [11, 25, 27, 31, 32, 33, 34] for examples of BCF-type models.

For a one-step system, we consider an adatom density, $c(x,t)$, that obeys

$$\partial_t c(x,t) = \mathcal{D}\partial_x^2 c(x,t), \tag{1.2}$$

where $\mathcal{D}$ is a (constant) diffusivity and $0 \le x < \varsigma(t)$, $\varsigma(t) < x \le L$, where $\varsigma(t)$ is the step position (cf. Figure 1(b)). We apply periodic boundary conditions in the

[6] Our T-matrix can be rewritten as a stochastic transition matrix $\mathbf{P}$ (a nonnegative matrix with rows or columns summing to one, depending on convention) via $\mathbf{T} = \mathbf{P} - \mathbf{I}$, where $\mathbf{I}$ is the identity matrix.

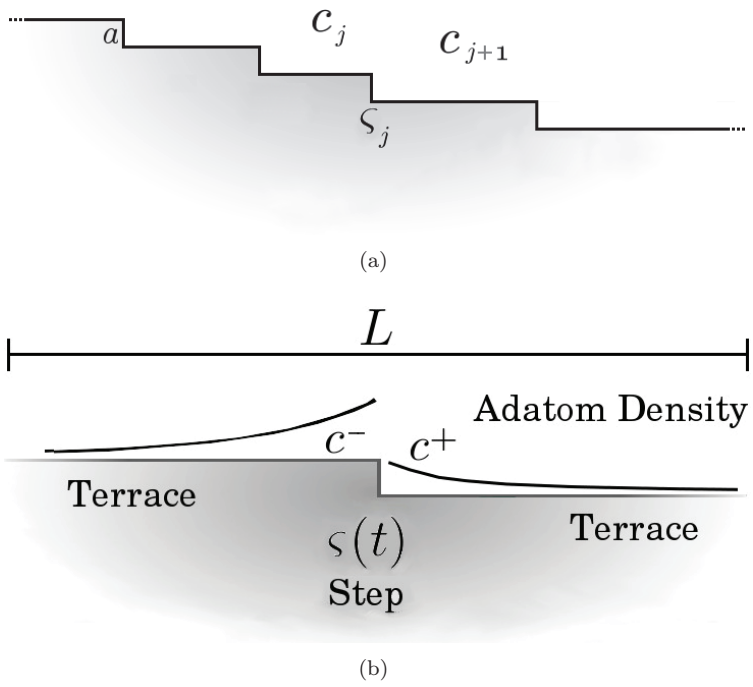

FIG. 1. (a) *A generic, 1D step system with multiple steps (with positions ς_j) separating terraces. Adatoms, represented by the densities c_j, diffuse on each terrace. The velocity of a step is proportional to the net current of adatoms arriving at the step. In general, the adatom densities need not be continuous across a step. In the BCF model, steps, which are an atomic length a in height, are defined as elements of the model from the outset.* (b) *The single-step system that we consider. The step position is denoted $\varsigma(t)$. The values $c^{\pm}$ are the adatom densities on the right (+) and left (−) sides of the step; L is the length of the system.*

coordinate x. Boundary conditions at the step are [18]

$$J_{\pm} = -\mathcal{D}\partial_x c\big|_{\pm} = \mp\kappa_{\pm}(c^{\pm} - c^{\mathrm{eq}}), \qquad x = \varsigma(t), \tag{1.3}$$

where $J_{\pm}$ is the adatom flux at the right (+) or left (−) edge of the step, $\kappa_{\pm}$ is an attachment/detachment rate at the right (+) or left (−) edge of the step,[7] and $c^{\pm}$ is the adatom concentration to the right (+) or left (−) of the step. The term c^{eq} is an equilibrium adatom concentration. *One of our goals is to derive an expression having the form of* (1.3)*, which allows us to express k and c^{eq} in terms of parameters of the atomistic, KMC model.*

Because the step moves, we require an additional equation in order to close the system. Let $\dot{\varsigma}(t)$ denote the step velocity and set it equal to the net flux,

$$\dot{\varsigma}(t) = a(J_- - J_+), \tag{1.4}$$

where a is the (atomic) height of the step. Equation (1.4) can be viewed as a statement about mass conservation: adatoms diffusing to a step attach to or detach from it, which causes the step to advance or retreat.

[7] The original BCF formulation [5] amounts to $\kappa_{\pm} \to \infty$, so that $c = c^{\mathrm{eq}}$ at the step edge.

In our analysis, we use the term "discrete BCF equations" to refer to (1.2)–(1.4), with the derivatives in x replaced by finite differences in the lattice site. The step-continuum theory comes from taking the limit as the lattice spacing approaches zero.

1.2. Past works. Several works have addressed questions related to the connection between atomistic surface models and BCF-type theories. We now frame our analysis in the context of those studies.

In [1], the authors derive linear kinetic relations analogous to (1.3) for a two-dimensional (2D) surface. We note three differences between their analysis and ours.

(i) In [1], the authors focus on the effects of external material deposition, which we leave out.

(ii) In [1], the solution to the discrete diffusion equation (atomistic model) is the set of probabilities that an adatom is found at each lattice site, irrespective of the position of all other adatoms; correlations are not considered. In contrast, the solution to our KMC model is the set of joint probabilities of finding adatoms at different locations on the surface, which explicitly includes correlations. In section 6, we show that these correlations give rise to correction terms in the BCF model.

(iii) In [1], the step position is fixed. Here, we view the step as a reservoir that can always move by emitting (or absorbing) adatoms.

In [53] and [26], the authors use a 2D KMC master equation to derive a modified diffusion equation that accounts for adatom interactions on a terrace and external material deposition. However, they do not derive a step velocity law or linear kinetic relation. An important part of their analysis is to represent the atomistic states as sets of discrete height columns and then average over the heights of those columns. This procedure removes the notion of discrete changes in height associated with steps (see Figure 1(a)). We, on the other hand, do not average over heights, and we explicitly define steps in our analysis.

In [38], the authors compare KMC simulations with the predictions of the BCF model for a system with external material deposition. The authors find the best agreement between the two models when detachment from the step is switched off in the KMC simulations. We speculate that including both external material deposition and detachment in the KMC model could lead to conditions in which the surface is not in the low-density regime. In particular, whenever the ratio $FL^2/(Da)$ is sufficiently large (where F is the deposition rate and a is the atomic length), we expect that corrections to the BCF theory will be nonnegligible, since adatoms will not have time to diffuse to the step before another deposition event occurs (cf. [30]). Note that in [39], the author implicitly compares the predictions of KMC simulations to a linear stability analysis of a BCF-type step-flow model.

1.3. Limitations. In this work, we focus exclusively on a system with a single step for mathematical convenience. However, we expect that including more steps will not affect our main conclusion. In particular, the BCF theory should be a consequence of the low-density approximation (i.e., no correlations), which we will show to be valid for one-step systems that are sufficiently close to equilibrium. If one considers multistep systems, Boltzmann statistics imply that the probability of finding many adatoms on the surface should scale as $e^{-E_b n/k_B T}$, which is independent of the number of steps on the surface. Consequently, we expect that the low-density approximation also applies to multistep systems as a condition for the validity of the BCF theory.

Because we limit ourselves to one dimension, our analysis ignores any effects due to the 2D step geometry; including such effects presents many additional complications to our model. For example, it is reasonable to expect that the attachment/detachment

kinetics at a 2D step depends on the local step curvature, which can lead to nontrivial effects (cf., for example, [33, 42]). In order to derive this result from an atomistic model, we would first need to formulate an appropriate master equation that accounts for both the 2D step position and the number of adatoms on the surface. However, a 2D step position has a much larger configuration space compared to our 1D system, for which the number and positions of adatoms are the only degrees of freedom. Moreover, averaging in two dimensions introduces new challenges, since it might be necessary to take expectation values over atomistic configurations that include variations of the step profile due to kinks (cf. [1]). We leave such issues for future work.

1.4. Structure of the paper. The remainder of the paper is organized as follows. In section 2, we introduce some notation. In section 3, we present numerical results of KMC simulations that suggest a correspondence between the KMC and BCF models. In section 4, we formulate the m-p model and apply the low-density approximation in order to derive the 1-p model. In section 5, we derive discrete BCF equations from the 1-p model. In section 6, we extend this derivation to the m-p model and show how the continuum BCF equations, with corrections, arise from the atomistic perspective. In section 7, we discuss our results in the context of variations on our KMC formulation and real material systems, and we outline limitations of the model and pose open questions.

2. Terminology and notation. An *edge atom* has the properties that (i) it has only one in-plane nearest neighbor, which is to its left; and (ii) all atoms to its left have two in-plane neighbors; see Figure 2(a).

A *step atom* has the properties that (i) it has two in-plane nearest neighbors, and (ii) all atoms to its left have two in-plane nearest neighbors; see Figure 2(a).

An *adatom* is a particle that is neither a step atom nor an edge atom; see Figure 2(a).

We say that an adatom attaches to a step when it moves to the lattice site directly to the right of an edge atom; this adatom then becomes an edge atom. We say that an edge atom detaches from the step and becomes an adatom when it moves to either of its adjacent lattice sites; see Figure 2(b).

A terrace site is any lattice site that is not directly to the right of an edge atom; see Figure 3.

A few comments on the notation are in order.

(i) We use j as an Eulerian coordinate to represent lattice sites in one dimension and $\mathfrak{j}$ as a Lagrangian coordinate to represent the position of a single adatom.

(ii) Lowercase bold letters (such as $\boldsymbol{\alpha}$ and $\mathfrak{a}$) represent multisets whose *unordered* elements denote the positions of *indistinguishable* adatoms.[8]

(iii) $\boldsymbol{\alpha}$ is an Eulerian coordinate, and $\mathfrak{a}$ is the corresponding Lagrangian coordinate in a setting where more than one adatom exist on the surface.

(iv) $|\boldsymbol{\alpha}|$ is the cardinality of multiset $\boldsymbol{\alpha}$. (However, $|x|$ denotes the absolute value of the real number x, as usual.)

(v) The symbol $\{\}$ represents the empty set, $\emptyset$.

(vi) $\boldsymbol{\alpha} \setminus \boldsymbol{\alpha'}$ denotes the multiset difference, or the elements of $\boldsymbol{\alpha}$ that are not contained in $\boldsymbol{\alpha'}$, including multiplicity (i.e., $\{1,1,2\} \setminus \{1,2,3\} = \{1\}$).

(vii) $||\boldsymbol{\alpha}||$ is the Euclidean norm of $\boldsymbol{\alpha}$, i.e., $||\boldsymbol{\alpha}|| = \left(\sum_j j^2\right)^{1/2},\ j \in \boldsymbol{\alpha}$.

[8] Note that the use of multisets (as opposed to ordered sets) is convenient for our purposes, since it avoids the need to count permutations of particle positions.

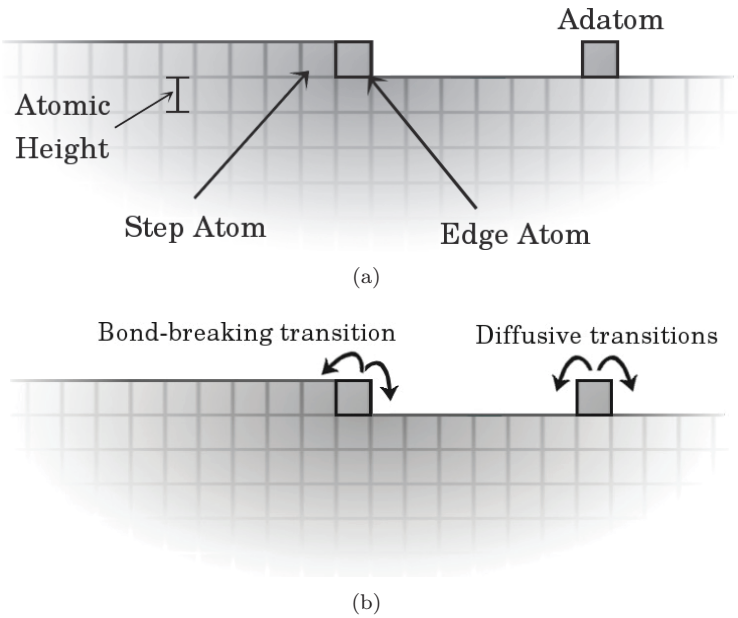

FIG. 2. (a) *KMC perspective of a* 1*D surface. Atoms, confined to a lattice, are the only elements of the model; they are classified according to the number of in-plane nearest-neighbor bonds that they have. In this perspective, the step is not a natural element of the model, but instead must be defined in terms of adatom configurations (cf. section* 1.4*).* (b) *Transitions in a KMC model. In our formulation, only adatoms and edge atoms are allowed to move, corresponding to the diffusive and bond-breaking transitions illustrated above.*

(viii) Matrices are denoted by uppercase, bold letters (e.g., $\boldsymbol{T}$) and the corresponding matrix elements with subscripted letters (e.g., $T_{i,j}$).

(ix) $T_{\boldsymbol{\alpha},\boldsymbol{\alpha}'}$ extends the notation of a matrix element to multisets.

(x) $\mathbb{1}_{\boldsymbol{\alpha}}(x) = y$ if x appears y times in $\boldsymbol{\alpha}$. Note that $\mathbb{1}_{\boldsymbol{\alpha}}(x)$ is not the standard definition of the set indicator function. We omit the subscript $\boldsymbol{\alpha}$ when the multiset being referenced is clear from context.

(xi) Summation is implied over repeated indices unless otherwise noted.

3. Correspondence between KMC and BCF: Numerical results. Our goal in this section is to motivate the idea that KMC models are a plausible microscopic perspective from which to derive the BCF theory. We perform a series of KMC simulations and qualitatively show that their predictions are consistent with those of the BCF theory. This exposition is divided into two subsections. In section 3.1, we outline the simulation algorithm and describe the essential physics of our KMC model, and in section 3.2, we discuss our numerical results.

3.1. KMC simulations. We consider a 1D surface with N height columns that are one atomic length a wide and whose heights are defined relative to a fixed plane of atoms. The columns are indexed by j, where $0 \le j \le N-1$; 0, 1, or more atoms may reside in each column. If $\mathfrak{m}$ atoms are in the same column, they form a stack (starting from the column base) that is $\mathfrak{m}$ atomic lengths high (cf. Figure 3). Thus, the coordinates j and $\mathfrak{m}$ define a 2D grid, and the number of atoms on any square of that grid is either 0 or 1. We impose screw periodic boundary conditions; for example, if an adatom hops to the right from the $(N-1)$th height column, it arrives at the

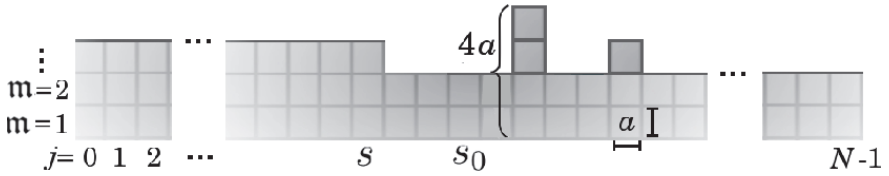

FIG. 3. *Schematic of the system in our 1D KMC simulations. The index j, $0 \le j \le N-1$, labels height columns, and the index $\mathfrak{m}$ labels height, $\mathfrak{m} \ge 1$. Each ordered pair $(j, \mathfrak{m})$ corresponds to a square whose sides are an atomic length a. At most one atom may occupy any such square. There are three adatoms on the surface. The microscopic step position is denoted s. We use s_0 to denote the step position $s + |\boldsymbol{\alpha}|$, where $|\boldsymbol{\alpha}|$ is the number of adatoms on the surface. Every lattice site except for $j = s + 1$ is part of the terrace.*

0th height column. We henceforth refer to the height columns indexed by j as lattice sites.

We take the total number of atoms in the system to be $\mathcal{O}(N)$. These atoms are grouped into one of three classes: step atoms, edge atoms, or adatoms (cf. Figure 2(a) and section 1.4). All atoms in a given class are otherwise indistinguishable. We place an immobile atom directly to the left of $(j, \mathfrak{m}) = (0, 1)$ so that an atom at $(0, 1)$ is always either an edge or step atom. The *microscopic* step position $s(t)$, which is a function of the number of *adatoms* on the surface, is defined to be the lattice site (i.e., height column) where the edge atom is found (cf. Figure 3). We denote s_0 as the location of the step when all atoms are step or edge atoms, i.e., when there are no adatoms on the surface.

The state of the system is uniquely determined by the position of all *adatoms*, and the system transitions from one state to another when one of the following three events happens: (i) an adatom moves, (ii) an edge atom detaches from the step, or (iii) an adatom attaches to the step. Whenever an edge atom detaches from (or an adatom attaches to) the step, the step site moves to the left (right) by one lattice site.

We describe our KMC algorithm through the following set of rules.

RULE 1. *An atom is only allowed to horizontally move a distance of one lattice site at a given time; the stack from which (to which) the atom moves changes in height by $-a$ $(+a)$.*

RULE 2. *In any height column with at least one adatom, the topmost adatom hops from a terrace site to any adjacent terrace site with a probability proportional to a constant rate D (described below), independent of the number of adatoms occupying the ending sites (i.e., adatoms can hop to occupied sites); no atoms below the topmost adatom of that column may move.*

RULE 3. *An adatom hops from the left $(-)$ or right $(+)$ of the step to the site directly to the right of the step with probability proportional to an attachment rate $D\phi_\pm$ (defined in* (3.2)*), provided the process creates only a single-step atom.*

RULE 4. *An edge atom is allowed to detach from a step to the left $(-)$ or right $(+)$ with probability proportional to a detachment rate $Dk\phi_\pm$ (defined in* (3.2) *and* (3.1)*), provided the process creates exactly one adatom.*

RULE 5. *Processes that convert a step atom into an adatom (or vice versa) are forbidden.*

See Figure 4 for an illustration of Rules 2–4 and section 6.2 for a discussion of the processes forbidden by Rule 5.

Physically, the parameter D corresponds to a hopping transition rate, i.e., the inverse of the expectation time for an adatom to hop on the terrace. For our purposes,

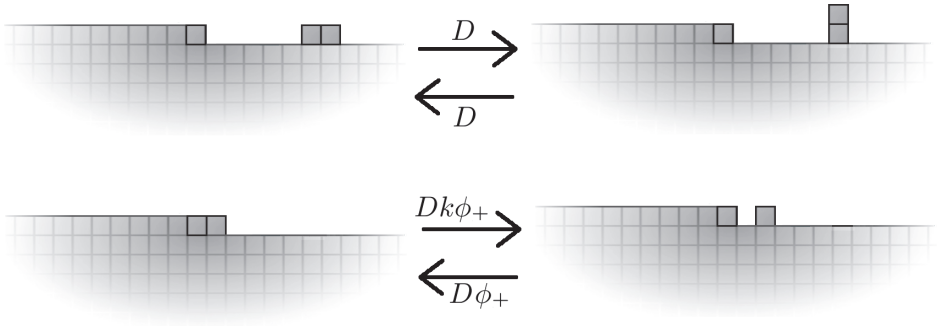

FIG. 4. *Illustration of transitions between atomistic configurations via Rules* 2–4 *of our KMC model. (Top) Adatoms hop to adjacent terrace sites at a rate* D*. On the top-right, only the topmost adatom may move (cf. Rule* 2*). (Bottom) An edge atom detaches at a rate* $Dk\phi_+$*, while an adatom attaches to the step at a rate* $D\phi_+$ *(cf. Rules* 3 *and* 4*).*

it suffices to assume that $D \geq \mathcal{O}(N^2)$ s^{-1}, which often holds for real materials [18]. The parameters k and $\phi_\pm$ are Arrhenius factors that account for the extra time needed to break a bond and attach to a step, respectively. We assume that

$$k = e^{-E_b/k_B T}, \tag{3.1}$$

$$\phi_\pm = e^{-E_\pm/k_B T}, \tag{3.2}$$

where $E_\pm \geq 0$ and $E_b > 0$ are the attachment and bond energy barriers, respectively; E_- is sometimes referred to as the "Ehrlich–Schwoebel barrier" [9, 40]. Each of these barriers can be up to a few tenths of an eV, so that for temperatures up to roughly 1000 K, the values for $\phi_\pm$ and k can range from 10^{-1} to 10^{-6} or smaller, depending on the material. See [2, 15, 50] for a discussion on the physical assumptions underlying D, $\phi_\pm$, and k; see also section 7.1.

In practice, the set of Rules 1–5 are implemented by a computer using random number generators. Given a starting configuration, a single particle (from the allowed set) is moved with a probability proportional to its transition rates. The amount of simulation time attributed to each individual process is chosen randomly from a Poisson distribution whose mean is the inverse of the transition rate for that process [2, 50]. Iterating this algorithm evolves the system. For each set of parameters $E_\pm$, E_b, and T, we run between 10^6 and 10^8 simulations (each having between 1 and about 1000 Monte Carlo steps) and calculate (i) the average microscopic step position, (ii) the average number of adatoms j sites away from the step (for $1 \leq j \leq N-1$), and (iii) the average flux of adatoms to the right side of the step edge. Each realization begins in an initial configuration in which all atoms are attached to the step.

Remark 3.1. Rule 2 amounts to neglecting the bonds between adatoms; however, it does allow for steric hindrance of motion, since only the topmost adatom in a column is allowed to hop. In one dimension, the presence of nearest-neighbor adatom bonds can lead to steady states in which the probability of an island nucleating is independent of its size. However, in two dimensions, Boltzmann statistics for a KMC scheme show that large islands are less probable than small islands (see section 7.2). Our assumption that adatoms do not interact via bonding is meant to render our analysis more consistent with 2D systems while avoiding subtleties associated with nucleation in 1D. See section 7.2 for a discussion of this issue; also see [3, 10] for

works related to nucleation in one dimension.

Remark 3.2. Rules 3–5 imply that a step can never move by more than one lattice site at a time. While this assumption is not necessary for the purposes of our derivation, it simplifies the formulation of our master equation. See section 7.2 for a discussion on variations of the master equation that allow for more general types of step motion.

Remark 3.3. It is expected that the probabilities of finding the system in an atomistic configuration numerically converge to an equilibrium Boltzmann distribution in the long-time limit. See, e.g., [23] for a discussion on how KMC simulations approach equilibrium.

3.2. Simulation results. In Figures 5 and 6, we show KMC results for our 1D surface with one step. In all simulations we fixed $k_BT = 1/40$ eV ($T \approx 273$ K), $D = 10^{10}$ s^{-1}, and $N = 50$.

Figure 5 shows the average number $n_j(t)$ of adatoms that are j lattice sites away from the step at six successive times. Since the index j is always measured relative to the step (regardless of the number of adatoms on the surface), we set the step position to be $j = 0$. By screw periodic boundary conditions, $j = 0$ and $j = 50$ correspond to the same lattice site.

In Figure 6(a), we plot the flux of atoms to the right of the step versus time. In Figure 6(b), we plot this flux versus the number of adatoms n_1 to the right of the step. We emphasize five important features of Figures 5 and 6.

Remark 3.4. Figure 5 shows that, on average, adatoms detach from a step and diffuse toward the middle of the terrace. At long times the system approaches an equilibrium in which the mean number of adatoms at a particular site is the same for all sites. This behavior is consistent with (1.2).

Remark 3.5. In Figure 6(b), the average flux at the step is approximately linear in the average number of adatoms n_1 over seven orders of magnitude of flux values. Moreover, the magnitude of the slope of the corresponding curve is of order D, where $D = 10^{10}$ s^{-1}, i.e., very large compared to N^2 s^{-1}. This behavior is consistent with the linear kinetic relation (1.3) when κ is large. We return to this point in section 6.4.

Remark 3.6. In Figure 6(b), the average flux vanishes when the average number of adatoms at the step goes to k; cf. (3.1). This result suggests that c^{eq} in (1.3) can be identified with k/a, where a is the atomic spacing; see section 6.

Remark 3.7. In Figure 5, the average number of adatoms at the step edge reaches its equilibrium value on a timescale that is much shorter than the time for the system to reach equilibrium. In light of Remarks 3.5 and 3.6, this behavior is reminiscent of diffusion limited kinetics.

Remark 3.8. Figures 5 and 6 show that in equilibrium, the probability of finding an adatom that is j sites from the step is $n_j(t\to\infty) \approx k = e^{-E_b/(k_BT)}$. Note that

$$n_j(t\to\infty) := \sum_{\boldsymbol{\alpha}} \chi(\boldsymbol{\alpha}, j) e^{-E_b n(\boldsymbol{\alpha})/(k_BT)} \approx e^{-E_b/(k_BT)}, \tag{3.3}$$

where summation is over all possible states $\boldsymbol{\alpha}$, the total number of adatoms in state $\boldsymbol{\alpha}$ is $n(\boldsymbol{\alpha})$, and $\chi(\boldsymbol{\alpha}, j)$ is the number of adatoms j sites away from the step for state $\boldsymbol{\alpha}$. *Since we identify E_b as the energy cost to create a single adatom, we conclude that n_j is dominated entirely by the* 1*-p states.* This observation is central to our analysis.

4. KMC master equation. Our goal in this section is to formulate a plausible, analytic framework from which we can derive the BCF theory. We begin by considering the m-p model, which is an analytic version of the KMC algorithm of section 3.

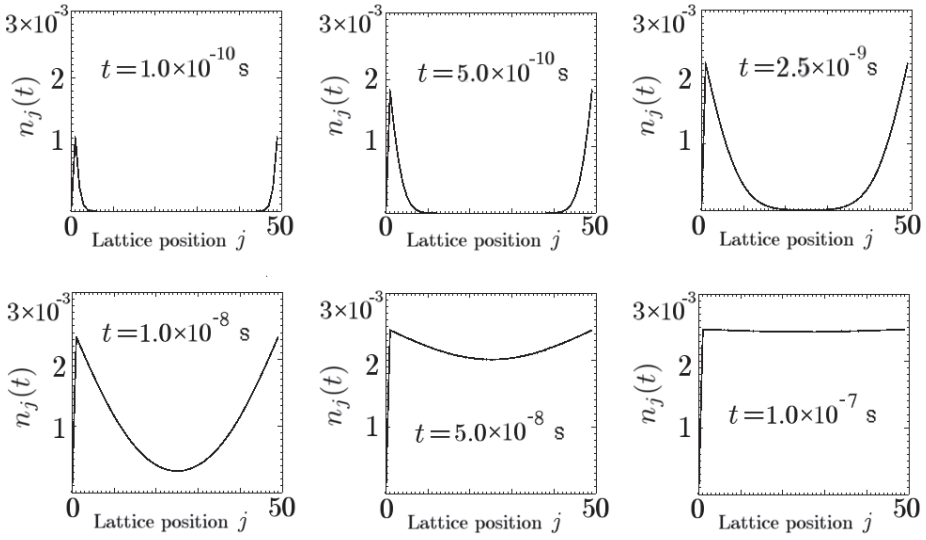

FIG. 5. *Average number of adatoms at a given lattice site, relative to the step, for six different times during a KMC simulation. We take the mean of* 10 *ensemble averages, with each ensemble consisting of* 10^7 *simulations (for a total of* 10^8 *simulations). The standard deviation of the* 10 *ensemble averages, which determines the error bars, is not visible because it is less than the thickness of each curve. The system is* 50 *lattice sites wide, and the step is always taken to be at the zeroth (or leftmost) lattice site. We use* $E_b = 0.15$ *eV,* $E_\pm = 0$ *eV,* $k_BT = 1/40$ *eV,* $D = 10^{10}$ s^{-1}*, and* $N = 50$*. The average number of adatoms directly to the right of the step reaches its equilibrium value fast relative to the timescale over which the system equilibrates. This behavior is reminiscent of diffusion limited kinetics* [18].

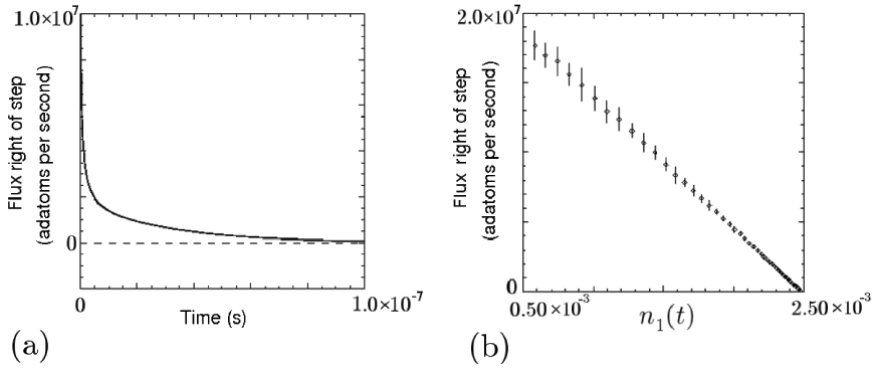

FIG. 6. (a) *Average flux of atoms to the right of the step versus time. Positive values correspond to net detachment of particles.* (b) *Average flux of atoms at the right of the step versus the probability* n_1 *of finding an adatom at* $j = 1$*. In both figures, we take the mean of* 10 *ensemble averages, with each ensemble consisting of* 10^7 *simulations (for a total of* 10^8 *simulations). In* (a)*, the error bars are not visible because the standard deviation* σ *of the* 10 *ensemble averages is less than the thickness of the curve; in* (b)*, the* 3σ *values are indicated by vertical lines centered at the mean flux values. We set* $E_b = 0.15$ *eV,* $E_\pm = 0$ *eV,* $k_BT = 1/40$ *eV,* $D = 10^{10}$ s^{-1}*, and* $N = 50$*. Note that for* $n_1 \approx k = \exp(-E_b/k_BT)$*, the flux of atoms goes to zero, which suggests that a corresponding equilibrium density* c^{eq} *in the BCF theory should be proportional to* k*. As a function of* n_1*, the flux is approximately linear in a certain regime of adatom probabilities.*

Motivated by Remark 3.8, we show that the m-p model may be cast into the form of a BBGKY-type hierarchy whose first equation describes the motion of a single adatom; this equation reduces to the 1-p model by application of the low-density approximation. We isolate the 1-p model in particular because it contains the essential elements of the BCF theory in a simple form (cf. section 5).

4.1. M-p model. We begin with an analytic model that allows more than one atom to move on the surface. We use the setting of section 3; cf. Figure 3.

4.1.1. General case. Consider the system described in section 3.1, and let $\boldsymbol{\alpha}$ be a multiset whose elements denote the positions of $|\boldsymbol{\alpha}| \leq m$ adatoms. Any element $j \in \boldsymbol{\alpha}$ records the location of one of the m adatoms, where $0 \leq j \leq N-1$. Moreover, the elements $j \in \boldsymbol{\alpha}$ may have a multiplicity greater than 1; the multiplicity of j is equal to the number of adatoms at the lattice site j. Since the location of all adatoms contains all of the information about the system, we call $\mathfrak{a} = \boldsymbol{\alpha}$ the system *state*.

Our KMC model analytically expresses the rules of section 3.1 via a system of ordinary differential equations (ODEs), a master equation.

DEFINITION 4.1 (m-p model). *Let $p_{\boldsymbol{\alpha}}(t)$ be the probability that there are adatoms occupying the sites given by $\boldsymbol{\alpha}$, where $|\boldsymbol{\alpha}| \leq m$. This $p_{\boldsymbol{\alpha}}$ satisfies the ODEs*

$$\dot{p}_{\boldsymbol{\alpha}} = T_{\boldsymbol{\alpha},\boldsymbol{\alpha}'} p_{\boldsymbol{\alpha}'} \tag{4.1}$$

for $t > 0$. These ODEs are supplemented by screw periodic boundary conditions and the initial data $p_{\boldsymbol{\alpha}}(0)$, which satisfies $\sum_{\boldsymbol{\alpha}} p_{\boldsymbol{\alpha}}(0) = 1$. The matrix $\mathbf{T} = [T_{\boldsymbol{\alpha},\boldsymbol{\alpha}'}]$ has the following properties:

$$T_{\boldsymbol{\alpha},\boldsymbol{\alpha}'} = 0 \quad \text{if } |\boldsymbol{\alpha}| = |\boldsymbol{\alpha}'|,\ |\boldsymbol{\alpha} \backslash \boldsymbol{\alpha}'| = 1, \text{ and } \Big| ||\boldsymbol{\alpha} \backslash \boldsymbol{\alpha}'|| - ||\boldsymbol{\alpha}' \backslash \boldsymbol{\alpha}|| \Big| > 1, \tag{4.2}$$

$$T_{\boldsymbol{\alpha},\boldsymbol{\alpha}'} = 0 \quad \text{if } |\boldsymbol{\alpha}| = |\boldsymbol{\alpha}'| \text{ and } |\boldsymbol{\alpha} \backslash \boldsymbol{\alpha}'| > 1, \tag{4.3}$$

$$T_{\boldsymbol{\alpha},\boldsymbol{\alpha}'} = 0 \quad \text{if } \Big| |\boldsymbol{\alpha}| - |\boldsymbol{\alpha}'| \Big| > 1, \tag{4.4}$$

$$T_{\boldsymbol{\alpha},\boldsymbol{\alpha}'} = D \quad \text{if } |\boldsymbol{\alpha}| = |\boldsymbol{\alpha}'|,\ |\boldsymbol{\alpha} \backslash \boldsymbol{\alpha}'| = 1, \text{ and } \Big| ||\boldsymbol{\alpha} \backslash \boldsymbol{\alpha}'|| - ||\boldsymbol{\alpha}' \backslash \boldsymbol{\alpha}|| \Big| = 1, \tag{4.5}$$

$$T_{\boldsymbol{\alpha},\boldsymbol{\alpha}'} = Dk\phi_{\pm} \quad \text{if } |\boldsymbol{\alpha}| - |\boldsymbol{\alpha}'| = 1 \text{ and } \boldsymbol{\alpha} \setminus \boldsymbol{\alpha}' = \{s_0 - |\boldsymbol{\alpha}'| \pm 1\}, \tag{4.6}$$

$$T_{\boldsymbol{\alpha},\boldsymbol{\alpha}'} = 0 \quad \text{if } |\boldsymbol{\alpha}| - |\boldsymbol{\alpha}'| = 1 \text{ and } \boldsymbol{\alpha} \setminus \boldsymbol{\alpha}' \neq \{s_0 - |\boldsymbol{\alpha}'| \pm 1\}, \tag{4.7}$$

$$T_{\boldsymbol{\alpha},\boldsymbol{\alpha}'} = D\phi_{\pm} \quad \text{if } |\boldsymbol{\alpha}'| - |\boldsymbol{\alpha}| = 1 \text{ and } \boldsymbol{\alpha}' \setminus \boldsymbol{\alpha} = \{s_0 - |\boldsymbol{\alpha}| \pm 1\}, \tag{4.8}$$

$$T_{\boldsymbol{\alpha},\boldsymbol{\alpha}'} = 0 \quad \text{if } |\boldsymbol{\alpha}'| - |\boldsymbol{\alpha}| = 1 \text{ and } \boldsymbol{\alpha}' \setminus \boldsymbol{\alpha} \neq \{s_0 - |\boldsymbol{\alpha}| \pm 1\}, \tag{4.9}$$

$$T_{\boldsymbol{\alpha},\boldsymbol{\alpha}} = -\sum_{\substack{\boldsymbol{\alpha}' \\ \boldsymbol{\alpha}' \neq \boldsymbol{\alpha}}} T_{\boldsymbol{\alpha}',\boldsymbol{\alpha}} \quad \text{for all } \boldsymbol{\alpha}. \tag{4.10}$$

Equations (4.2)–(4.10) have interpretations in terms of Rules 1–5. Equations (4.2) and (4.3) state that only one adatom may move at a time, and in this process, it may only move a distance of one lattice site (Rule 1). Equation (4.4) states that no process may create or destroy more than one adatom (Rule 5; cf. also Remark 3.2). Equation (4.5) states that adatoms hop between terrace sites at a constant rate D (Rule 2). Equations (4.6) and (4.7) state that edge atoms detach to the right or left at a constant rate $Dk\phi_{\pm}$ (Rule 4). Equations (4.8) and (4.9) state that adatoms attach to the step from the right or left at a constant rate $D\phi_{\pm}$ (Rule 3). Equation (4.10) ensures that probability is conserved or, equivalently, that $\sum_{\boldsymbol{\alpha}} \dot{p}_{\boldsymbol{\alpha}} = 0$.

Evidently, the parameter s_0 is the location of the edge atom when there are no adatoms on the surface. Thus, $s_0 - |\mathfrak{a}|$ measures the position of the edge atom relative

to the state {} (when the edge atom is at s_0). Equations (4.6) and (4.8) therefore account for bonding at the edge atom site when multiple adatoms are on the surface.[9]

Remark 4.2. The m-p model is ergodic; i.e., any state $\mathfrak{a}' = \boldsymbol{\alpha}'$ can be reached from any other state $\mathfrak{a} = \boldsymbol{\alpha}$ in a finite number of transitions; see Lemma A.3 of Appendix A for a basic proof.

Remark 4.3. The T-matrix given by (4.2)–(4.10) satisfies the Kolmogorov criterion, which states that, for any closed loop in state space, $(\mathfrak{a} = \boldsymbol{\alpha}) \to (\mathfrak{a}' = \boldsymbol{\alpha}') \to (\mathfrak{a}'' = \boldsymbol{\alpha}'') \to \cdots \to (\mathfrak{a}''' = \boldsymbol{\alpha}''') \to (\mathfrak{a} = \boldsymbol{\alpha})$, the product of rates in the forward direction equals the product of rates in the reverse direction. That is, if $T_{\boldsymbol{\alpha},\boldsymbol{\alpha}'}$ is the transition rate from state $\mathfrak{a}' = \boldsymbol{\alpha}'$ to state $\mathfrak{a} = \boldsymbol{\alpha}$ (cf. (4.24)), then $T_{\boldsymbol{\alpha}',\boldsymbol{\alpha}}T_{\boldsymbol{\alpha}'',\boldsymbol{\alpha}'}\cdots T_{\boldsymbol{\alpha},\boldsymbol{\alpha}'''} = T_{\boldsymbol{\alpha}''',\boldsymbol{\alpha}}\cdots T_{\boldsymbol{\alpha}',\boldsymbol{\alpha}''}T_{\boldsymbol{\alpha},\boldsymbol{\alpha}'}$ (summation not implied); see Lemma A.4 of Appendix A for a basic proof. Notably, the Kolmogorov criterion implies that the transition rates obey detailed balance [7].

Remark 4.4. The ergodicity property of (4.2)–(4.10) and the fact that the T-matrix satisfies the Kolmogorov criterion are sufficient to ensure that any set of real initial data $p_{\boldsymbol{\alpha}}(0)$ approaches a unique steady state in the long-time limit (see Proposition A.5 of Appendix A).

4.1.2. An example: The two-particle (2-p) model. In this section, we give a specific example of an m-p model in which there are only *two* movable atoms in the entire system.

The multisets $\boldsymbol{\alpha}$ that label adatom configurations may have 0, 1, or 2 elements, which correspond to zero-particle (0-p), 1-p, or 2-p states; see Figure 7. We enumerate

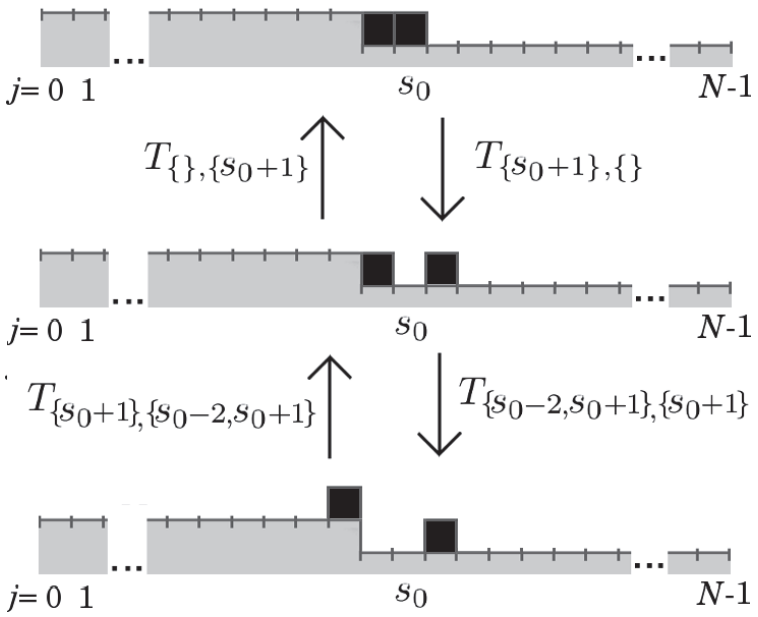

FIG. 7. *Schematic of* 2*-p model. Only two atoms are movable. Top:* 0*-p state (*$|\boldsymbol{\alpha}| = 0$*). Middle:* 1*-p state, for which* $|\boldsymbol{\alpha}| = 1$*. Bottom:* 2*-p state, for which* $|\boldsymbol{\alpha}| = 2$*. The elements of the T-matrix that describe the transition rates between the illustrated states are written next to arrows indicating the direction of the transition. See also* (4.11).

[9]Because the form of the T-matrix (4.2)–(4.10) is translation invariant in s_0, the step velocity laws that we derive in sections 5 and 6 are independent of s_0.

all of the nonzero, off-diagonal matrix elements of $T_{\boldsymbol{\alpha},\boldsymbol{\alpha}'}$:

$$
\begin{aligned}
&(4.11a) && T_{\{s_0\pm1\},\{\}} = Dk\phi_\pm, && && (0\text{-p} \to 1\text{-p transition})\\
&(4.11b) && T_{\{\},\{s_0\pm1\}} = D\phi_\pm, && && (1\text{-p} \to 0\text{-p})\\
&(4.11c) && T_{\{j\},\{j\pm1\}} = D, && j, j\pm1 \neq s_0, && (1\text{-p} \to 1\text{-p})\\
&(4.11d) && T_{\{j,s_0-1\pm1\},\{j\}} = Dk\phi_\pm, && j \neq s_0-1, s_0, && (1\text{-p} \to 2\text{-p})\\
&(4.11e) && T_{\{j\},\{j,s_0\}} = D\phi_+, && j \neq s_0-1, s_0, && (2\text{-p} \to 1\text{-p})\\
&(4.11f) && T_{\{j\},\{j,s_0-2\}} = D\phi_-, && j \neq s_0-1, s_0, && (2\text{-p} \to 1\text{-p})\\
&(4.11g) && T_{\{j,k\},\{j,k\pm1\}} = D, && j \neq s_0-1, && (2\text{-p} \to 2\text{-p})\\
& && && k, k\pm1 \neq s_0-1. &&
\end{aligned}
$$

4.1.3. M-p model as a BBGKY-type hierarchy. As section 4.1.2 illustrates, it is possible to separate the system states into a hierarchy based on the number of adatoms $|\mathfrak{a}|$ in state $\mathfrak{a}$. In general, we write

$$
\dot{p}_{\boldsymbol{\alpha}} = \sum_{\substack{\boldsymbol{\alpha}'\\ |\boldsymbol{\alpha}'|=|\boldsymbol{\alpha}|-1}} T_{\boldsymbol{\alpha},\boldsymbol{\alpha}'}p_{\boldsymbol{\alpha}'} \;+\; \sum_{\substack{\boldsymbol{\alpha}'\\ |\boldsymbol{\alpha}'|=|\boldsymbol{\alpha}|}} T_{\boldsymbol{\alpha},\boldsymbol{\alpha}'}p_{\boldsymbol{\alpha}'} \;+\; \sum_{\substack{\boldsymbol{\alpha}'\\ |\boldsymbol{\alpha}'|=|\boldsymbol{\alpha}|+1}} T_{\boldsymbol{\alpha},\boldsymbol{\alpha}'}p_{\boldsymbol{\alpha}'}. \tag{4.12}
$$

Equation (4.12) is a BBGKY-type hierarchy that connects the time evolution of an $|\boldsymbol{\alpha}|$-adatom joint probability to the $(|\boldsymbol{\alpha}|-1)$- and $(|\boldsymbol{\alpha}|+1)$-adatom joint probabilities. Motivated by Remark 3.8, we explicitly write the equations for $|\mathfrak{a}| = 1$:

$$
\begin{aligned}
\dot{p}_{\{j\}} &= D[p_{\{j+1\}} - 2p_{\{j\}} + p_{\{j-1\}}] - Dk(\phi_+ + \phi_-)p_{\{j\}}\\
&\quad + D\phi_+p_{\{j,s_0\}} + D\phi_-p_{\{j,s_0-2\}}, \qquad j \neq 0, s_0, s_0\pm1, N-1, && (4.13)\\
\dot{p}_{\{s_0+1\}} &= D[k\phi_+p_{\{\}} - (1+\phi_+)p_{\{s_0+1\}} + p_{\{s_0+2\}}] - Dk(\phi_+ + \phi_-)p_{\{s_0+1\}}\\
&\quad + D\phi_+p_{\{s_0,s_0+1\}} + D\phi_-p_{\{s_0-2,s_0+1\}}, && (4.14)\\
\dot{p}_{\{s_0-1\}} &= D[k\phi_-p_{\{\}} - (1+\phi_-)p_{\{s_0-1\}} + p_{\{s_0-2\}}], && (4.15)\\
\dot{p}_{\{\}} &= D[\phi_-p_{\{s_0-1\}} - k(\phi_- + \phi_+)p_{\{\}} + \phi_+p_{\{s_0+1\}}]. && (4.16)
\end{aligned}
$$

Note that the terms $Dk(\phi_+ + \phi_-)p_{\{j\}}$ and $D\phi_+p_{\{j,s_0\}} + D\phi_-p_{\{j,s_0-2\}}$ in (4.13) (and the analogous terms in (4.14)) account for processes in which an adatom detaches from or attaches to the step.

Based on our numerical results in section 3, we expect that the system will predominantly reside in the 1-p states described by (4.13)–(4.16). Moreover, since (4.13) resembles a discrete diffusion equation (provided we ignore processes involving 2-p states), and (4.14)–(4.16) describe transitions at the step, we take these equations as a plausible starting point for our derivation of the BCF theory.

4.2. 1-p model. In this section, we define the 1-p model more precisely as coming from a truncation of the m-p model (section 4.1) at the level of the $|\mathfrak{a}| = 1$ states. Consider (4.13)–(4.16) and neglect all terms that contain (i) $p_{\boldsymbol{\alpha}}$, where $|\boldsymbol{\alpha}| = 2$, or (ii) $kp_{\boldsymbol{\alpha}}$, where $\boldsymbol{\alpha} \neq \{\}$. We replace the multiset notation $\boldsymbol{\alpha} = \{j\}$ with the index j and $\boldsymbol{\alpha} = \{\}$ with s_0. This truncation scheme amounts to the low-density approximation and produces the 1-p model as follows.

DEFINITION 4.5. *Let $p_j(t)$ be the probability that the atom is at site j. This $p_j(t)$ is the solution to the 1-p model if*

$$
\dot{p}_j = D[p_{j+1} - 2p_j + p_{j-1}], \qquad j \neq 0,\ s_0, s_0\pm1,\ N-1, \tag{4.17}
$$

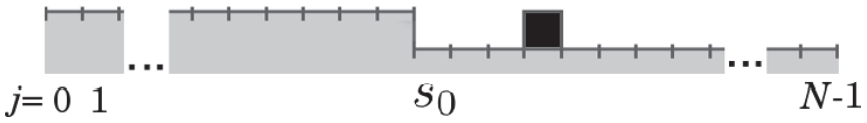

FIG. 8. *Schematic of 1-p model. Only a single particle is allowed to move on the surface, and it may occupy one of N lattice sites, indexed as* $0 \le j \le N-1$. *All other particles are fixed.*

$$\dot{p}_{s_0\pm1} = D[k\phi_\pm p_{s_0} - (1+\phi_\pm)p_{s_0\pm1} + p_{s_0\pm2}], \tag{4.18}$$

$$\dot{p}_{s_0} = D[\phi_- p_{s_0-1} - k(\phi_- + \phi_+)p_{s_0} + \phi_+ p_{s_0+1}] \tag{4.19}$$

for $t > 0$, *which are supplemented by the initial data* $p_j(0)$ *and the screw periodic boundary conditions,*

$$\dot{p}_0 = D[p_1 - 2p_0 + p_{N-1}], \tag{4.20}$$

$$\dot{p}_{N-1} = D[p_{N-2} - 2p_{N-1} + p_0], \tag{4.21}$$

where $p_j(0)$ *must satisfy*

$$\sum_{j=0}^{N-1} p_j(0) = 1. \tag{4.22}$$

By analogy to section 4.1.1, we denote the position of the moving atom by j, where $0 \le \mathrm{j} \le N-1$ (cf. Figure 8). We refer to the atom position j (which is a Lagrangian coordinate) as the system *state*, since j is the only element of the model that changes.

It is straightforward to show that the boundary conditions (4.20) and (4.21) imply $\sum_{j=0}^{N-1} \dot{p}_j = 0$, so that properly normalized initial data will remain so for all times $t > 0$. As we show in section 7.2, the details of the boundary conditions do not change the local behavior of the step, provided (4.22) remains true for all times $t > 0$.

Equations (4.17)–(4.21) may be written in the form

$$\dot{p}_j = T_{j,j'} p_{j'}, \tag{4.23}$$

where $T_{j,j'}$ is a matrix element that describes the transition rate from state $\mathrm{j}' = j'$ to state $\mathrm{j} = j$. The matrix elements are

$$\begin{aligned} T_{j,j'} = D\{&\delta_{j+1,j'}[1 + \delta_{j,s_0}(\phi_+ - 1) + \delta_{j+1,s_0}(k\phi_- - 1)] \\ &- \delta_{j,j'}[2 + \delta_{j,s_0}(\phi_+ + \phi_- - 2) + \delta_{j,s_0+1}(\phi_+ - 1) + \delta_{j,s_0-1}(\phi_- - 1)] \\ &+ \delta_{j-1,j'}[1 + \delta_{j,s_0}(\phi_+ - 1) + \delta_{j-1,s_0}(k\phi_+ - 1)]\}, \end{aligned} \tag{4.24}$$

where $\delta_{j,j'}$ is the Kronecker delta; i.e., $\delta_{j,j'} = 1$ if $j = j'$ and $\delta_{j,j'} = 0$ if $j \ne j'$.

Remark 4.6. Equations (4.17)–(4.21) imply ergodicity of the system; i.e., any state j' can be reached from any other state j in a finite number of transitions; see Lemma A.1 of Appendix A for a basic proof.

Remark 4.7. Equations (4.17)–(4.21) satisfy the Kolmogorov criterion [19, 22]. See Lemma A.2 of Appendix A for a basic proof.

Remark 4.8. The ergodicity of (4.17)–(4.21) and the fact that the T-matrix (4.24) satisfies the Kolmogorov condition are sufficient to ensure that any real initial data will evolve to a unique steady state at long times; see Proposition A.5 of Appendix A.

5. Averaging the 1-p model: Discrete BCF equations. Motivated by the results of section 3.2 and Remark 3.8, our goal in this section is to show that the 1-p model contains the essential elements of the BCF model. In this vein, we pursue the following tasks:

(i) define the step position and adatom density as averages over the probabilities $p_j(t)$ of the 1-p model (section 5.1);

(ii) show that the time evolution of these averages is described by a *discrete* second order difference scheme for the adatom density, a step velocity law (section 5.2);

(iii) derive a linear kinetic relation, *with corrections*, at the step edge (section 5.2); and

(iv) determine the conditions under which the corrections remain negligibly small for all $t > 0$ (section 5.3).

5.1. 1-p equilibrium solution: Notion of averaging. We use the notion of the equilibrium Boltzmann distribution to motivate definitions of the step position and adatom density for a system out of equilibrium [29].

We begin by setting $\dot{p}_j = 0$ in (4.17)–(4.21). By inspection we find that the steady state solution is $p_j^{\mathrm{eq}} = k/\mathcal{Z}$ for $j \neq s_0$ and $p_{s_0}^{\mathrm{eq}} = 1/\mathcal{Z}$, where $\mathcal{Z} = [(N-1)k + 1]$ is a normalization constant.[10] Noting that $k = \exp(-E_b/k_BT)$, we immediately conclude that p_j^{eq} is the Boltzmann distribution corresponding to our 1-p model; the steady state is equilibrium.

Hence, a natural definition of the equilibrium step position is

$$\varsigma^{\mathrm{eq}} := \left[\sum_{j\neq s_0} (s_0 - 1) a\, p_j^{\mathrm{eq}}\right] + s_0\, a\, p_{s_0}^{\mathrm{eq}}, \tag{5.1}$$

while the adatom density may be defined as

$$c_j^{\mathrm{eq}} := p_j^{\mathrm{eq}}/a, \quad j \neq s_0, \tag{5.2}$$

where $a = L/N$ and L is the linear size of the system. Note that the equilibrium adatom density is everywhere constant (cf. Figure 5).

We define the time-dependent step position and adatom density by replacing the equilibrium probabilities p_j^{eq} with $p_j(t)$ in expressions (5.1) and (5.2).

DEFINITION 5.1. *The step position $\varsigma(t)$ and adatom density $c_j(t)$ are defined as*

$$\varsigma(t) := \left[\sum_{j\neq s_0} a(s_0 - 1) p_j(t)\right] + a s_0 p_{s_0}(t), \tag{5.3}$$

$$c_j(t) := p_j(t)/a, \quad j \neq s_0, \tag{5.4}$$

for all $t \geq 0$.

By Remark 4.8, $\varsigma(t)$ and $c_j(t)$ are guaranteed to converge to their equilibrium values given by (5.1) and (5.2). Hence, we view (5.3) and (5.4) as the simplest expressions for the step position and adatom density that are consistent with equilibrium statistical mechanics. Note that (5.3) is the expectation value of the *microscopic* step position defined in section 3.1. In the context of our master equation perspective, we believe that (5.3) is the first instance of an analytic definition of a step.

Remark 5.2. We always assume that $N\exp(-E_b/k_BT) = Nk \ll 1$. This may be viewed as either a low-temperature or high-bond energy limit of the system. Recalling

[10] $\mathcal{Z}$ is in fact the partition function [29].

that $\mathcal{Z} = (N-1)k + 1$, one finds that $p_{s_0}^{\mathrm{eq}} = 1/\mathcal{Z} = 1 - \mathcal{O}(Nk)$ and $p_j^{\mathrm{eq}} = k/\mathcal{Z} = k - \mathcal{O}(Nk^2)$ for $j \neq s_0$. That is, the low-temperature limit also corresponds to a low-density limit of the system, insofar as in equilibrium, the atom remains attached to the step with a probability approximately equal to 1; see also section 5.3.

5.2. Evolution laws for averaged quantities. Next, we derive evolution laws for (5.3) and (5.4). Applying a time derivative to (5.3) and noting that the sum over (4.17) is telescoping, we find

$$\dot{\varsigma}(t) = a^2 D\phi_-(c_{s_0-1} - kp_{s_0}/a) + a^2 D\phi_+(c_{s_0+1} - kp_{s_0}/a). \tag{5.5}$$

The differences $c_{s_0\pm1} - kp_{s_0}/a$ are proportional to the flux of adatoms to site s_0, and the step velocity is given by the difference of adatom fluxes at the step.

Equation (4.17) is already a discrete adatom diffusion equation, so that we need only to derive boundary conditions at the step edge. We first write (4.18) in the same form as (4.17) plus a remainder term,

$$\dot{c}_{s_0\pm1} = D(c_{s_0}^{\pm} - 2c_{s_0\pm1} + c_{s_0\pm2}) + D[(1-\phi_\pm)c_{s_0\pm1} + (k\phi_\pm)p_{s_0}/a - c_{s_0}^{\pm}], \tag{5.6}$$

where we introduce the new variables $c_{s_0}^{\pm}$, which we interpret as the right (+) or left (−) density at the step edge. We identify these densities $c_{s_0}^{\pm}$ as the discrete analogues of $c^{\pm}$ appearing in (1.3).

By setting

$$D[c_{s_0\pm1} - c_{s_0}^{\pm}] = D\phi_\pm[c_{s_0\pm1} - kp_{s_0}/a], \tag{5.7}$$

we cast (5.6) into the same form as (4.17) and determine a set of boundary conditions for the adatom density at the step edge.[11]

To interpret the quantities appearing in (5.7), we compare this equation with (1.3). On the left-hand side of (5.7), we identify

$$\mathcal{J}_\pm := aD(c_{s_0\pm1} - c_{s_0}^{\pm}) \tag{5.8}$$

as the discrete flux to the step edge. On the right-hand side of (5.8), we assume that $c_{s_0\pm1} \approx c_{s_0}^{\pm}$ when $a = L/N$ is small.

Caution should be exercised in comparing the term kp_{s_0}/a of (5.7) with the c^{eq} of the BCF theory. In (1.3), c^{eq} is a reference density against which $c_{s_0}^{\pm}$ is measured. If the $c_{s_0}^{\pm}$ equals c^{eq}, then no current flows to or from the step. Moreover, this reference density should be defined for a system in equilibrium.

Microscopically, this idea corresponds to a detailed balance of flux at the step edge. Specifically, in (4.18), if $p_{s_0\pm1} = k/\mathcal{Z}$ and $p_{s_0} = 1/\mathcal{Z}$, then no probability current flows to or from the step. *In the KMC model, the reference density is simply proportional to the rate k at which atoms detach from the step,* provided k is small. This idea is further reinforced by the usual definition that $c^{\mathrm{eq}} \propto \exp(-\mu/k_BT)$, where the chemical potential μ is the energy cost of adding an adatom to the surface. In the KMC model, this cost is precisely E_b. Hence, we define the discrete equilibrium density as

$$\breve{c}^{\mathrm{eq}} := k/a. \tag{5.9}$$

[11] Note that (5.7) adds two additional equations (corresponding to $c_{s_0}^{\pm}$) to the system (4.17)–(4.21).

On the right-hand side of (5.7), this $\breve{c}^{\rm eq}$ is multiplied by p_{s_0}. However, we recall that when $kN \ll 1$, the equilibrium solution $p_{s_0} = 1 - \mathcal{O}(Nk)$. Therefore, we postulate that whenever the system is sufficiently close to equilibrium, we can replace $kc_{s_0} \to k/a + L^{-1}\mathcal{O}[(Nk)^2]$ and neglect the correction term. Under this assumption, we write

$$\mathcal{J}_\pm = Da\phi_\pm[c_{s_0\pm1} - k/a] + (Da^2/L^2)\mathcal{O}[(Nk)^2] \sim Da\phi_\pm[c_{s_0\pm1} - \breve{c}^{\rm eq}], \tag{5.10}$$

which is a discretized version of (1.3).

Remark 5.3. Unlike the correction terms that we consider in section 6, the $\mathcal{O}[(Nk)^2]$ term in (5.10) is due to memory effects, not multi-adatom correlations. Indeed, by integrating (4.19), we obtain

$$p_{s_0}(t) = D\int_0^t \mathrm{d}t' e^{-Dk(\phi_- + \phi_+)(t-t')}[\phi_- p_{s_0-1}(t') + \phi_+ p_{s_0+1}(t')]. \tag{5.11}$$

The value of p_{s_0} that multiplies k/a in (5.7) depends on the history of p_{s_0-1} and p_{s_0+1}. Physically, we interpret this to mean that the rate of detachment from a step depends on whether an edge atom is actually available to detach.

5.3. Maximum principle for 1-p model. In this section, we discuss a simple maximum principle that specifies a class of initial data for which $c_{s_0} = \mathcal{O}[(a\mathcal{Z})^{-1}]$ for all times. When this condition is satisfied, we define the system as being "near equilibrium." If, in addition, $Nk \ll 1$ (i.e., in the low-temperature regime), then $kc_{s_0} = k/a - L^{-1}\mathcal{O}[(Nk)^2]$, and we can ignore the correction terms in (5.7).

PROPOSITION 5.4. *Let $p_j(t)$ be the solution to* (4.17)–(4.21) *with initial data $p_j(0)$, and define $\hat{p}_j = p_j/k$ for $j \neq s_0$ and $\hat{p}_{s_0} = p_{s_0}$. Then $\hat{p}_j$ satisfies the maximum principle that $\max_j\{\hat{p}_j(t)\} \leq \max_j\{\hat{p}_j(0)\}$ for all $t > 0$.*

See Appendix B for a complete proof.

COROLLARY 5.5. *If $p_j(0) \leq \mathcal{O}(k)$ for $j \neq s_0$ and $p_{s_0}(0) = \mathcal{O}(1)$, then $p_j(t) \leq \mathcal{O}(k)$ for $j \neq s_0$ and $p_{s_0}(t) = \mathcal{O}(1)$ for all times t.*

DEFINITION 5.6. *Whenever $p_j(0)$ satisfies the hypotheses of Corollary* 5.5*, we define the state of the system to be near equilibrium.*

Corollary 5.5 specifies the conditions under which (5.10) is a discrete linear kinetic relation to $\mathcal{O}(k)$; if the system starts in any configuration in which $p_{s_0} = \mathcal{O}(1)$, then corrections to the linear kinetic relation are always $\mathcal{O}[(Nk)^2]$.

6. Averaging of m-p model. In sections 4 and 5, we derived discrete BCF-type equations by (i) applying the low-density approximation (i.e., the truncation scheme) to the m-p model, and then (ii) averaging over the resulting 1-p probabilities. However, care should be exercised in deriving the continuum versions of (5.5) and (5.7). Specifically, we take the physically motivated perspective that the step position and adatom density are ensemble averages taken over all states $\mathfrak{a}$. By averaging the atomistic states *after truncation*, we leave out contributions that come from multi-particle states. These contributions are negligibly small, $\mathcal{O}[(Nk)^2]$, in the low-density regime.

In this section, we include the multi-particle states in the averaging process in order to capture corrections due to adatom correlations. In this vein, we reverse the approach of sections 4 and 5.1. First, we average the step position and adatom density over all states $\mathfrak{a}$, which reduces the m-p model to a 1-p model plus corrections (sections 6.1 and 6.2). Second, by generalizing the maximum principle of section 5.3, we determine a criterion under which the corrections remain small for all times (section 6.3). Finally, the step continuum theory emerges in the limit that the lattice spacing goes to zero (section 6.4).

6.1. M-p model: Averaging revisited. In this section, we define the step position and adatom density for the m-p model by averaging over all states $\mathfrak{a}$; cf. (6.2) and (6.3). We begin by finding the equilibrium solution of the m-p model. Examination of (4.2)–(4.10) reveals that $\dot{p}_{\boldsymbol{\alpha}} = 0$ implies that the steady state solution is $p^{\text{eq}}_{\boldsymbol{\alpha}} = k^{|\boldsymbol{\alpha}|}/\mathcal{Z}$ for all $\boldsymbol{\alpha}$, where

$$\mathcal{Z} := 1 + k\left(\sum_{\substack{\boldsymbol{\alpha}\\ |\boldsymbol{\alpha}|=1}} 1\right) + k^2\left(\sum_{\substack{\boldsymbol{\alpha}\\ |\boldsymbol{\alpha}|=2}} 1\right) + \cdots + k^m\left(\sum_{\substack{\boldsymbol{\alpha}\\ |\boldsymbol{\alpha}|=m}} 1\right). \tag{6.1}$$

Noting that $k^{|\boldsymbol{\alpha}|} = \exp(-|\boldsymbol{\alpha}|E_b/k_BT)$, where $|\boldsymbol{\alpha}|$ is the number of adatoms in state $\boldsymbol{\alpha}$, we again conclude that the steady state solution of the m-p model is in fact the equilibrium solution, consistent with Boltzmann statistics.

By analogy to (5.3) and (5.4), we define the following time-dependent expectation values for the step position and adatom density.

DEFINITION 6.1. *The step position $\varsigma(t)$ and adatom density $c_j(t)$ at the jth lattice site away from the step are defined as*

$$\varsigma(t) := \left[\sum_{\boldsymbol{\alpha}} a\ (s_0 - |\boldsymbol{\alpha}|)\, p_{\boldsymbol{\alpha}}(t)\right], \tag{6.2}$$

$$c_j(t) := \sum_{\substack{\boldsymbol{\alpha}\\ s_0-|\boldsymbol{\alpha}|+1+j\in\boldsymbol{\alpha}}} p_{\boldsymbol{\alpha}}(t)/a \tag{6.3}$$

for all $t > 0$.

As in section 5, $a = L/N$. In the long-time limit, these expectation values converge to the m-p analogues of (5.1) and (5.2).

Remark 6.2. Equation (6.3) is the expectation value of finding *at least* one adatom that is j sites from the step. This definition does not coincide with the conventional notion of a particle density, since $|\boldsymbol{\alpha}|$ does not multiply $p_{\boldsymbol{\alpha}}$. On the other hand, (6.3) is appropriate for a KMC scheme in which only one particle is allowed to move at any given time, regardless of how many adatoms occupy a given site. See section 7.4 for a discussion of this point.

Remark 6.3. If $Nk \ll 1$, then by (6.1), one finds $\mathcal{Z} = 1 - \mathcal{O}(Nk)$. In equilibrium the probability that all atoms are attached to the step is $p_{\{\}} = 1 - \mathcal{O}(Nk)$.

6.2. Discrete BCF equations from the m-p model. In this section we derive evolution laws for the (time-dependent) step position and adatom density. The procedure for deriving the step velocity law is the same as in section 5.2; we apply a time derivative to (6.2) and use (4.2)–(4.10) to simplify the resulting expression. This yields

$$\begin{aligned}\dot{\varsigma}(t) &= Da^2[\phi_+ c_1(t) + \phi_- c_{-1}(t) - (\phi_- + \phi_+)(k/a)]\\ &\quad - Da\sum_{\boldsymbol{\alpha}\in\mathcal{F}_a^+}\phi_+ p_{\boldsymbol{\alpha}} \ - \ Da\sum_{\boldsymbol{\alpha}\in\mathcal{F}_a^-}\phi_- p_{\boldsymbol{\alpha}} \ + \ Da\sum_{\boldsymbol{\alpha}\in\mathcal{F}_d} k(\phi_+ + \phi_-)p_{\boldsymbol{\alpha}},\end{aligned} \tag{6.4}$$

where the sets $\mathcal{F}_a^{\pm}$ and $\mathcal{F}_d$ are defined as

$$\mathcal{F}_a^+ := \{\boldsymbol{\alpha} :\ \mathbb{1}(s_0 - |\boldsymbol{\alpha}| + 2) \geq 2\}, \tag{6.5}$$

$$\mathcal{F}_a^- := \{\boldsymbol{\alpha} :\ \mathbb{1}(s_0 - |\boldsymbol{\alpha}| + 2) \geq 1,\ \mathbb{1}(s_0 - |\boldsymbol{\alpha}|) \geq 1\}, \tag{6.6}$$

$$\mathcal{F}_d := \{\boldsymbol{\alpha} :\ s_0 - |\boldsymbol{\alpha}| \in \boldsymbol{\alpha} \text{ or } |\boldsymbol{\alpha}| = m\}. \tag{6.7}$$

Equations (6.5)–(6.7) define the sets of states in which attachment to the step from the right ($\mathcal{F}_a^+$), attachment from the left ($\mathcal{F}_a^-$), and detachment ($\mathcal{F}_d$) are forbidden; cf. Rule 5 (section 3.1) and Figure 9. By virtue of (6.3) (the definition for $c_j(t)$), such forbidden transitions are included in the first line of step velocity law (6.4), so that the second line is necessary to remove them.

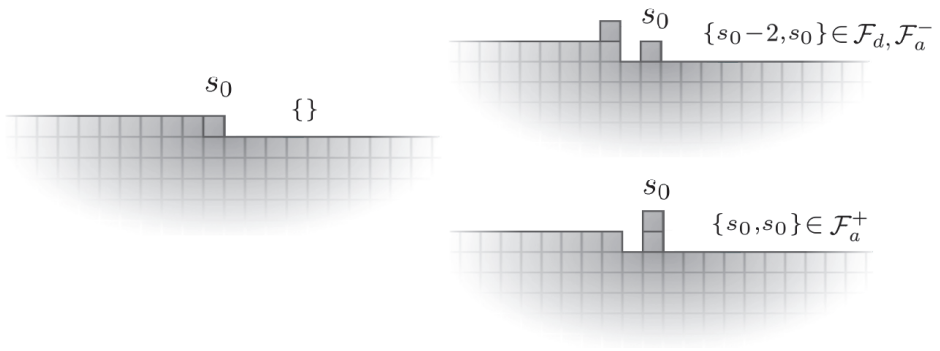

FIG. 9. *Illustration of forbidden transitions in our KMC model. The state* {} *on the left may not transition to the states* $\{s_0-2,s_0\}$ *or* $\{s_0,s_0\}$ *on the right. More generally, the model forbids processes in which* (i) *a step atom moves, or* (ii) *two or more step atoms are created; see also* (6.5)–(6.7).

In order to derive the discrete adatom diffusion equation, we apply a time derivative to (6.3) for $j\neq\pm1$ and again use (4.2)–(4.10) to simplify the resulting expression. By letting $\tilde{p}_{\boldsymbol{\alpha}}=p_{\boldsymbol{\alpha}}/a$, we find

$$\begin{aligned}\dot{c}_j(t) &= D[c_{j+1}-2c_j+c_{j-1}]\\ &\quad - D\sum_{\boldsymbol{\alpha}\in\mathcal{U}_j^-}\tilde{p}_{\boldsymbol{\alpha}}+2D\sum_{\boldsymbol{\alpha}\in\mathcal{U}_j}\tilde{p}_{\boldsymbol{\alpha}}-D\sum_{\boldsymbol{\alpha}\in\mathcal{U}_j^+}\tilde{p}_{\boldsymbol{\alpha}}\\ &\quad - D\sum_{\boldsymbol{\alpha}\in\mathfrak{D}_j}k(\phi_++\phi_-)\tilde{p}_{\boldsymbol{\alpha}}\ +\ D\sum_{\boldsymbol{\alpha}\in\mathcal{A}_{j+1}^+}\phi_+\tilde{p}_{\boldsymbol{\alpha}}\ +\ D\sum_{\boldsymbol{\alpha}\in\mathcal{A}_{j+1}^-}\phi_-\tilde{p}_{\boldsymbol{\alpha}}\\ &\quad + D\sum_{\boldsymbol{\alpha}\in\mathfrak{D}_{j-1}}k(\phi_++\phi_-)\tilde{p}_{\boldsymbol{\alpha}}\ -\ D\sum_{\boldsymbol{\alpha}\in\mathcal{A}_j^+}\phi_+\tilde{p}_{\boldsymbol{\alpha}}\ -\ D\sum_{\boldsymbol{\alpha}\in\mathcal{A}_j^-}\phi_-\tilde{p}_{\boldsymbol{\alpha}},\end{aligned}\tag{6.8}$$

where the sets $\mathcal{U}_j$, $\mathcal{U}_j^\pm$, $\mathfrak{D}_j$, and $\mathcal{A}_j^\pm$ are defined as

$$\mathcal{U}_j:=\{\boldsymbol{\alpha}:\ \mathbb{1}(s_0-|\boldsymbol{\alpha}|+1+j)\geq 2\},\tag{6.9}$$

$$\mathcal{U}_j^+:=\{\boldsymbol{\alpha}:\ s_0-|\boldsymbol{\alpha}|+1+j\in\boldsymbol{\alpha},s_0-|\boldsymbol{\alpha}|+2+j\in\boldsymbol{\alpha}\},\tag{6.10}$$

$$\mathcal{U}_j^-:=\{\boldsymbol{\alpha}:\ s_0-|\boldsymbol{\alpha}|+j\in\boldsymbol{\alpha},s_0-|\boldsymbol{\alpha}|+1+j\in\boldsymbol{\alpha}\},\tag{6.11}$$

$$\mathfrak{D}_j:=\{\boldsymbol{\alpha}:\ s_0-|\boldsymbol{\alpha}|+j+1\in\boldsymbol{\alpha},s_0-|\boldsymbol{\alpha}|\notin\boldsymbol{\alpha}\},\tag{6.12}$$

$$\mathcal{A}_j^+:=\{\boldsymbol{\alpha}:\ s_0-|\boldsymbol{\alpha}|+j+1\in\boldsymbol{\alpha},\mathbb{1}(s_0-|\boldsymbol{\alpha}|+2)=1\},\tag{6.13}$$

$$\mathcal{A}_j^-:=\{\boldsymbol{\alpha}:\ s_0-|\boldsymbol{\alpha}|+j+1\in\boldsymbol{\alpha},s_0-|\boldsymbol{\alpha}|\in\boldsymbol{\alpha},s_0-|\boldsymbol{\alpha}|+2\notin\boldsymbol{\alpha}\}.\tag{6.14}$$

The set $\mathcal{U}_j$ contains all states $\mathfrak{a}$ in which two or more adatoms are at site j (relative to the step), while the sets $\mathcal{U}_j^\pm$ are those sets in which an adatom is at site j, and another adatom is at $j\pm1$. The set $\mathfrak{D}_j$ contains all states with an adatom at j and an edge atom that may detach from the step. The sets $\mathcal{A}_j^\pm$ contain the states with an

adatom at j and another adatom which is able to attach to the step from the left ($-$) or right ($+$). By virtue of (6.3), transitions between state $\mathfrak{a} \in \mathcal{U}_j$ and state $\mathfrak{a}' \in \mathcal{U}_j^{\pm}$ (where $T_{\boldsymbol{\alpha},\boldsymbol{\alpha}'} \neq 0$) leave the value of $c_j(t)$ unchanged; thus, the second line of (6.8) removes such transitions from (6.8) (see also Figure 10 and Remark 6.2). The third and fourth lines of (6.8) account for the fact that the density $c_j(t)$ (cf. (6.3)) changes whenever the step moves, since the adatom positions are always measured relative to the step; see also Figure 11.

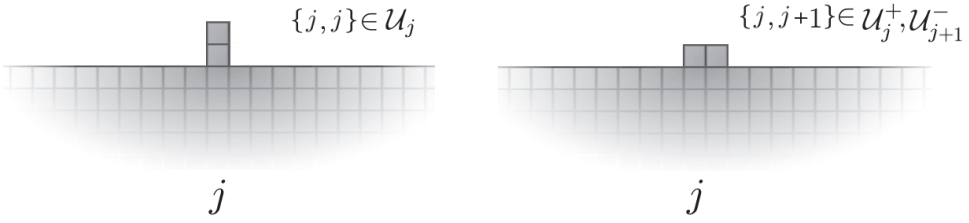

FIG. 10. *Transitions that leave the adatom density unchanged. The density $c_j(t)$ is not changed by any transition in which the lattice site j (relative to the step) is occupied by at least one adatom before and after the transition. The correction terms appearing in the second line of* (6.8) *remove such transitions from the equation for $\dot{c}_j$. See* (6.3) *and Remark* 6.2.

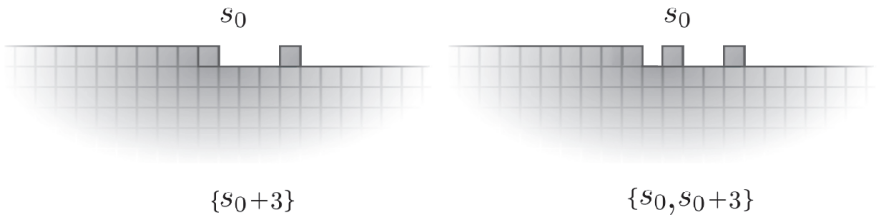

FIG. 11. *Schematic of the effect of step motion on adatom density. When a step moves via an attachment or detachment process, all adatoms change their position relative to the step. Hence, such transitions also change the density $c_j(t)$ (cf.* (6.3)*). The correction terms appearing in the third and fourth lines of* (6.8) *account for such changes.*

By applying a time derivative to $c_1(t)$, we find

$$\begin{aligned}\dot{c}_1(t) = {} & D[c_{s_0}^+ - 2c_1 + c_2] + D[c_1(1-\phi_+) + (k/a)\phi_+ - c_{s_0}^+] \\ & - D\sum_{\boldsymbol{\alpha}\in\mathcal{F}_d} k\phi_+\tilde{p}_{\boldsymbol{\alpha}} \;+\; D\sum_{\boldsymbol{\alpha}\in\mathcal{F}_a^+} \phi_+\tilde{p}_{\boldsymbol{\alpha}} \;+\; D\sum_{\boldsymbol{\alpha}\in\mathcal{U}_1} \tilde{p}_{\boldsymbol{\alpha}} \;-\; D\sum_{\boldsymbol{\alpha}\in\mathcal{U}_1^+} \tilde{p}_{\boldsymbol{\alpha}} \\ & - D\sum_{\boldsymbol{\alpha}\in\mathfrak{D}_1} k\phi_-\tilde{p}_{\boldsymbol{\alpha}} \;+\; D\sum_{\boldsymbol{\alpha}\in\mathcal{A}_2^+} \phi_-\tilde{p}_{\boldsymbol{\alpha}}, \end{aligned} \tag{6.15}$$

where the last two lines are correction terms accounting for processes that (i) are forbidden in our KMC rules (via $\mathcal{F}_d$ and $\mathcal{F}_a^+$), (ii) leave the density of adatoms unchanged (via $\mathcal{U}_1$ and $\mathcal{U}_1^+$), or (iii) cause the step to move (relative to the adatom) by means of a detachment ($\mathfrak{D}_1$) or attachment ($\mathcal{A}_2^+$) process. As in section 5.2, the density $c_{s_0}^+$ is a new variable that we introduce in order to make the evolution equation for $\dot{c}_1(t)$ take the same form as (6.8). We therefore assume that

$$D[c_1(1-\phi_+) + (k/a)\phi_+ - c_{s_0}^+] - D\sum_{\boldsymbol{\alpha}\in\mathcal{F}_d} k\phi_+\tilde{p}_{\boldsymbol{\alpha}} \;+\; D\sum_{\boldsymbol{\alpha}\in\mathcal{F}_a^+} \phi_+\tilde{p}_{\boldsymbol{\alpha}} = 0, \tag{6.16}$$

which determines the boundary condition for c_1 at the right of the step; we group the correction terms associated with forbidden processes with the kinetic relation (6.16), since these are the same correction terms appearing in (6.4).

Similarly, by applying a time derivative to $c_{-1}(t)$ we find

$$\begin{aligned}\dot{c}_{-1}(t) = {} & D[c^-_{s_0} - 2c_{-1} + c_{-2}] + D[c_{-1}(1-\phi_-) + (k/a)\phi_- - c^-_{s_0}] \\ & - D\sum_{\boldsymbol{\alpha}\in\mathcal{F}_d} k\phi_-\tilde{p}_{\boldsymbol{\alpha}} \;+\; Da\sum_{\boldsymbol{\alpha}\in\mathcal{F}_a^+}\phi_-\tilde{p}_{\boldsymbol{\alpha}} \;+\; D\sum_{\boldsymbol{\alpha}\in\mathcal{U}_{-1}}\tilde{p}_{\boldsymbol{\alpha}} \;-\; D\sum_{\boldsymbol{\alpha}\in\mathcal{U}^-_{-1}}\tilde{p}_{\boldsymbol{\alpha}} \\ & + D\sum_{\boldsymbol{\alpha}\in\mathfrak{D}_{-2}} k\phi_+\tilde{p}_{\boldsymbol{\alpha}} \;-\; D\sum_{\boldsymbol{\alpha}\in\mathcal{A}^+_{-1}}\phi_+\tilde{p}_{\boldsymbol{\alpha}}. \qquad (6.17)\end{aligned}$$

The correction terms in the second and third lines of (6.17) have interpretations similar to those appearing in (6.15); we use $c^-_{s_0}$ in the same way as $c^+_{s_0}$, i.e., to make (6.17) have the same form as (6.8). To find a boundary condition for $c_{-1}(t)$, we set

$$D[c_{-1}(1-\phi_-) + (k/a)\phi_- - c^-_{s_0}] - D\sum_{\boldsymbol{\alpha}\in\mathcal{F}_d} k\phi_-\tilde{p}_{\boldsymbol{\alpha}} \;+\; Da\sum_{\boldsymbol{\alpha}\in\mathcal{F}_a^+}\phi_-\tilde{p}_{\boldsymbol{\alpha}} = 0. \qquad (6.18)$$

Remark 6.4. All of the correction terms appearing in (6.4)–(6.18) either contain probabilities $p_{\boldsymbol{\alpha}}$, with $|\boldsymbol{\alpha}| \geq 2$, or are proportional to $kp_{\boldsymbol{\alpha}}$, with $|\boldsymbol{\alpha}| \geq 1$. By the maximum principle of section 6.3, these corrections are all negligibly small.

6.3. Maximum principle for the m-p model. In this section, we determine a set of near-equilibrium conditions ensuring that the correction terms appearing in (6.8)–(6.17) remain small for all times $t > 0$. To this end, we present a generalization of Proposition 5.4.

PROPOSITION 6.5. *Assume that $p_{\boldsymbol{\alpha}}(t)$ is the solution to $\dot{p}_{\boldsymbol{\alpha}}(t) = T_{\boldsymbol{\alpha},\boldsymbol{\alpha}'}p_{\boldsymbol{\alpha}'}(t)$, where $T_{\boldsymbol{\alpha},\boldsymbol{\alpha}'}$ is given by* (4.2)–(4.10) *(summation is implied over repeated multisets). Moreover, assume that $|\boldsymbol{\alpha}| \leq m$ for all $\boldsymbol{\alpha}$, where m is some positive integer, and define $\hat{p}_{\boldsymbol{\alpha}}(t) := p_{\boldsymbol{\alpha}}(t)/k^{|\boldsymbol{\alpha}|}$. Then $\hat{p}_{\boldsymbol{\alpha}}(t)$ satisfies the maximum principle that $\max_{\boldsymbol{\alpha}}\{\hat{p}_{\boldsymbol{\alpha}}(t)\} \leq \max_{\boldsymbol{\alpha}}\{\hat{p}_{\boldsymbol{\alpha}}(0)\}$ for all times $t > 0$.*

See Appendix B for a proof.

COROLLARY 6.6. *Assume that $p_{\boldsymbol{\alpha}}(0) \leq \mathcal{O}(k^{|\boldsymbol{\alpha}|})$. Then $p_{\boldsymbol{\alpha}}(t) \leq \mathcal{O}(k^{|\boldsymbol{\alpha}|})$ for all times t.*

DEFINITION 6.7. *Whenever the initial data satisfies $p_{\boldsymbol{\alpha}}(0) \leq \mathcal{O}(k^{|\boldsymbol{\alpha}|})$ according to Corollary* 6.6*, we define the state of the system to be near equilibrium. We refer to the hypotheses of Corollary* 6.6 *as "near-equilibrium conditions."*

Remark 6.8. Corollary 6.6 defines the conditions under which the discrete BCF equations are valid to $\mathcal{O}(k)$ for all times. Physically, these near-equilibrium conditions imply that whenever all of the probabilities $p_{\boldsymbol{\alpha}}(0)$ are close to the Boltzmann distribution, they remain so for all times $t > 0$.

6.4. Continuum limit of the m-p model. In this section, we formally derive the continuum limit of (6.4)–(6.17), which is a step continuum model in 1+1 dimensions, in the sense described in [18]. We begin with the assumption that as $a \to 0$, the function $\hat{p}_{\boldsymbol{\alpha}}(t) \to \hat{p}(\mathfrak{x}, t)$, where $\mathfrak{x}$ is an unordered multiset whose elements (which have units of length) may take any continuous value from 0 to L. We further assume that $\hat{p}_{\boldsymbol{\alpha}}(t) - \hat{p}_{\boldsymbol{\alpha}'}(t) = L^{-2}\mathcal{O}(a)$ for all $t > 0$ and all pairs $\boldsymbol{\alpha}$ and $\boldsymbol{\alpha}'$ (with $\boldsymbol{\alpha} \neq \boldsymbol{\alpha}'$) for which $T_{\boldsymbol{\alpha},\boldsymbol{\alpha}'} \neq 0$.[12]

[12] A rigorous proof of this claim would require a study of a priori estimates for the discrete equations, which we do not pursue here.

Under these assumptions, $c_j(t) \to c(x,t)$ where x is a continuous variable, and $0 \le x \le L$. Furthermore, as $a \to 0$ we find

$$\frac{c((j+1)a,t) - c(ja,t)}{a} = \partial_x c(x,t) + L^{-3}\mathcal{O}(a), \tag{6.19}$$

$$\frac{c((j+1)a,t) - 2c(ja,t) + c((j-1)a,t)}{a^2} = \partial_{xx} c(x,t) + L^{-4}\mathcal{O}(a). \tag{6.20}$$

Next, we set $\mathcal{D} = Da^2$, where $\mathcal{D}$ is a macroscopic diffusivity that should remain bounded as $N \to \infty$. We also impose the condition $0 < \mathcal{K} = Nk \ll 1$ as $N \to \infty$ and assume that the system is near equilibrium (cf. Remark 6.8). Under these assumptions, we find that step velocity law (6.4) is recast in the form

$$\dot{\varsigma}(t) = \mathcal{D}\phi_+(c^+ - c^{\mathrm{eq}}) + \mathcal{D}\phi_-(c^- - c^{\mathrm{eq}}) + (\mathcal{D}/L)\mathcal{O}(\mathcal{K}k). \tag{6.21}$$

In (6.21), we therefore identify $\mathcal{D}\phi_\pm$ as $a\kappa_\pm$, where a is the atomic length in the BCF model. In order to show that the correction is $\mathcal{O}(\mathcal{K}k)$, consider the second line of (6.4), for example, the term

$$Da \sum_{\boldsymbol{\alpha} \in \mathcal{F}_a^+} \phi_+ p_{\boldsymbol{\alpha}} \le DaC \sum_{n=2}^{n=m} N^{n-2} k^n = (\mathcal{D}/L)\mathcal{O}(\mathcal{K}k), \tag{6.22}$$

where C is some constant that is independent of $\mathcal{K}$ and k; see also Remark 6.4 and Proposition 6.5.

Under these assumptions, (6.8) becomes

$$\partial_t c(x,t) = \mathcal{D}\partial_{xx} c(x,t) + (\mathcal{D}/L^3)\mathcal{O}(\mathcal{K}^2). \tag{6.23}$$

To verify the size of the $\mathcal{O}(\mathcal{K}^2)$ correction, note that all of the corrections to (6.8) contain differences $p(\boldsymbol{\alpha}a,t) - p(\boldsymbol{\alpha}'a,t) = L^{-1}\mathcal{O}(ak^{|\boldsymbol{\alpha}|})$ for which $T_{\boldsymbol{\alpha},\boldsymbol{\alpha}'} \neq 0$. Consequently, we may write, for example,

$$-D \sum_{\boldsymbol{\alpha} \in \mathcal{U}_j^-} \tilde{p}_{\boldsymbol{\alpha}} + 2D \sum_{\boldsymbol{\alpha} \in \mathcal{U}_j} \tilde{p}_{\boldsymbol{\alpha}} - D \sum_{\boldsymbol{\alpha} \in \mathcal{U}_j^+} \tilde{p}_{\boldsymbol{\alpha}} \le (\mathcal{D}/L^3)\mathcal{O}(\mathcal{K}^2). \tag{6.24}$$

By applying the same arguments to (6.16) and (6.18), we find

$$J_\pm = -\mathcal{D}\partial_x c(x,t) = \mp\kappa_\pm(c^\pm - c^{\mathrm{eq}}) + (\mathcal{D}/L^2)\mathcal{O}(\mathcal{K}k), \tag{6.25}$$

where we identify $\kappa_\pm = Da\phi_\pm = \mathcal{D}\phi_\pm/a$ and $c^{\mathrm{eq}} = \mathcal{K}/L$.

As $a \to 0$, we find that $\kappa_\pm \to \infty$ provided $\phi_\pm$ remains bounded. Hence, our analysis implies that in the absence of an attachment barrier, i.e., $\phi_\pm = 1$, the system is in a diffusion limited regime, in which detachment from the step is a fast process relative to diffusion. If $\phi_\pm = \mathcal{O}(N^{-1})$ as $N \to \infty$, then $\kappa_\pm$ remains bounded, and the system moves into an attachment/detachment limited regime in which diffusion is the fastest process [16].

Remark 6.9. In Figure 12, we compare KMC simulations (described in section 3) with the linear kinetic relation (6.25). Notably, the simulations are in excellent agreement with our definitions of $\kappa_\pm$ and c^{eq} when c^+ is within about 20% of the value of c^{eq}. This range is consistent with our prediction that the BCF theory should approximate the KMC model whenever the system is near equilibrium, i.e., when $c = \mathcal{O}(c^{\mathrm{eq}})$.

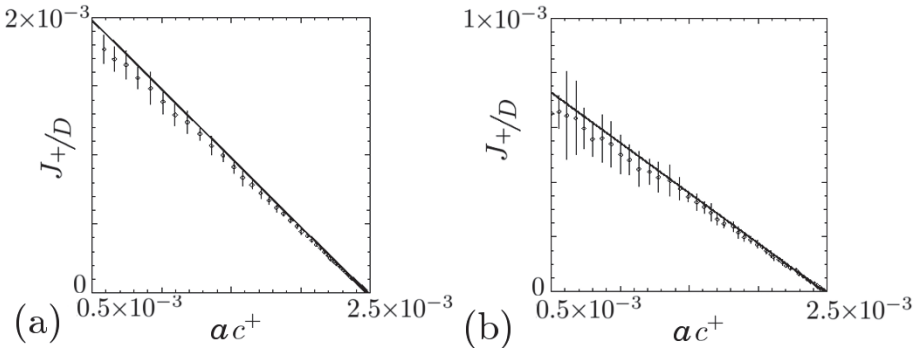

FIG. 12. *Linear kinetic relation* (6.25) *versus KMC simulations.* (a) *Simulations with* $\phi_+ = 1$, *i.e.,* $E_+ = 0$. (b) *Simulations with* $\phi_\pm = 1/e$, *i.e.,* $E_\pm/k_BT = 1$. *We take the mean of* 10 *ensemble averages, with each ensemble consisting of* (a) 10^7 *simulations, and* (b) 10^6 *simulations. The* 3σ *values are indicated by vertical lines (error bars) centered at the mean flux values. In both plots, we take* $k \approx 0.0025$, $D = 10^{10}\ s^{-1}$, *and* $N = 50$ *(so* $a = L/50$*); note that* $ac^{\mathrm{eq}} = k$. *The slopes of the solid lines are* (a) $J_+/[D(ac^+ - k)] = -1$, *and* (b) $J_+/[D(ac^+ - k)] = -1/e$, *in agreement with our BCF-type model.*

7. Discussion. In this section, we (i) consider our results in the context of experimental systems, (ii) review key assumptions underlying our KMC model and indicate why they are physically acceptable, (iii) explore implications for the quasi-static approach, and (iv) discuss limitations of our model.

7.1. Real material systems. In our analysis, we require that $D = \mathcal{O}(N^2)\ \mathrm{s}^{-1}$ and $Nk \ll 1$ as $N \to \infty$ in order to derive BCF equations in the continuum limit. The second condition ($Nk \ll 1$) in particular allows us to invoke the low-density approximation. In this section, we discuss the validity of these conditions in the context of real material systems.

The hopping rate D is usually defined as the Arrhenius function $D := f_h e^{-E_h/k_BT}$, where $f_h = 10^{13}\ \mathrm{s}^{-1}$ is an attempt frequency and E_h is an activation energy that is extracted from measurements [18]. Typical values for E_h range from 0.04 eV for Al(111) to 0.97 ± 0.07 eV for Si(111) [18]. At temperatures between 300 K and 1000 K, we estimate that $10^{12}\ \mathrm{s}^{-1} \geq D \geq 10^6\ \mathrm{s}^{-1}$, depending on the material. As an example, we consider Ni(110), for which $E_h = 0.41$ eV [18, 41]; taking $T \approx 500$ K (or $k_BT \approx 1/24$ eV), we estimate that $D = 10^8\ \mathrm{s}^{-1}$. For a terrace with $N = 1000$ lattice sites and $L = 0.1\ \mu$m (i.e., atomic length $a = 0.1$ nm), we find $\mathcal{D} = D/(a^2) = 1\ \mu\mathrm{m}^{-2}\ \mathrm{s}^{-1}$.

Experiments can also estimate the energy E_b (cf. (3.1)). Typical values range from approximately 0.3 eV for Ni(110) [41][13] up to 1 eV or 2 eV for Si(111) [20, 35, 36]. The use of the value $E_b = 0.3$ eV for Ni(110) (cf. (3.1)) yields $k \approx 10^{-4}$ at 500 K. By combining this result with the assumption that $N = 1000$ (corresponding to L that is a few hundred nanometers), we find that $Nk \approx 10^{-1}$, which suggests that the low-density approximation is reasonable for this system at 500 K. In addition to these formal estimates, both experimental and numerical results have verified that Ni(110) is in a low-density regime at this temperature; see [41]. In this work, significant adatom detachment on Ni(110) began only when the temperature was raised above

[13] In [41], the activation energy E_a for creating an adatom is equal to $E_h + E_b$ in our model. Note that $E_a \approx 0.7$ eV in [41] and $E_h \approx 0.4$ eV in [18, 41] yield $E_b \approx 0.3$ eV.

650 K; at 900 K, simulations show that roughly 1.5% of the lattice sites are occupied by adatoms (see also [14]).

Experimental estimates of $E_\pm$ are also available (cf. (3.2)). Often (but not always) the Ehrlich–Schwoebel barrier [9, 40] E_- is larger than the attachment barrier E_+. See, e.g., Table 6 in [18] for a detailed list of attachment/detachment barriers.[14] For Ni(110), one finds $E_- = 0.9$ eV and $E_+ \approx 0$ eV, which implies $\phi_- \ll 1/N$ and $\phi_+ = 1$ at 500 K. In a BCF model for this system, we therefore expect that $\kappa_- \approx 0$ and $\kappa_+ = \mathcal{O}(N)$, corresponding to $\mathcal{J}_- = 0$ and $c_+ = c^{\mathrm{eq}}$ (see section 6.4). Therefore, for this system our analysis predicts different boundary conditions on each side of the step edge.

For other works that consider the near-equilibrium conditions and adatom density in the context of semiconductors, see [24, 47].

7.2. Consequences of dimensionality. Rules 1–5 impose several restrictions on the allowed atomistic transitions. In this section, we briefly discuss the physical motivation of these restrictions as well as implications of relaxing them.

In both the KMC simulations of section 3 and master equation (4.2)–(4.10) of the m-p model, we ignore adatom-pair interactions; see Remark 3.1. If we relax this assumption by allowing nearest-neighbor adatom interactions, then the energy cost to make any island should be constant, irrespective of its size (cf. Figure 13); by Boltzmann statistics, all islands are equally probable at equilibrium. On the other hand, the probability of finding an island should decrease with its size (i.e., the number of broken bonds); see Figure 13. Therefore, we exclude adatom interactions in our 1D model on the grounds that such interactions do not capture the physics of island formation. Our model also neglects processes that allow steps to move by more than one lattice site at a time; see Remark 3.2. If we relax this assumption by allowing a step atom to move while still forbidding adatom interactions, the step atom must break $n+1$ bonds, where n is the number of atoms to the right of the moving atom. We forbid such processes on the grounds that they are unphysical, since the step atom has only two nearest-neighbor in-plane bonds. In a 2D setting, where it is reasonable to allow adatom interactions, the detachment of step atoms is a physically acceptable process because it breaks only nearest-neighbor bonds.

7.3. Implications for the quasi-static approach. Definition (6.3) measures the adatom density relative to the step position; consequently, our analysis takes place in a frame of reference that is comoving with the step. In such cases, we expect that (1.2) should contain a term proportional to $\dot{\varsigma}\partial_x c(x,t)$, which accounts for convection [12, 18, 32]. Inspection of (6.8) shows that convection-type events (where one adatom moves relative to the step when an edge atom detaches) appear only as corrections to our BCF-type model, not to leading order in $\mathcal{K}$. Physically this may be understood by noting that convection events necessarily involve two (or more) particle states, which are small for systems sufficiently close to equilibrium.

This observation implies that the step velocity $\dot{\varsigma}$ is slow relative to the timescale in which the system equilibrates, so that $\partial_t c(x,t) \approx 0$ for macroscopic times; often, this is called the *quasi-static regime* [18]. That the step velocity is small relative to the timescale of adatom diffusion may also be seen from (6.21). Specifically, the right-hand side of this equation behaves as $\mathcal{O}(1/N)$ for any values of $\phi_\pm \leq \mathcal{O}(1)$ and

[14] The attachment/detachment barriers in Table 6 of [18] are not the same as $E_\pm$ in (3.2). In [18], the definitions of $E_{a,u}$ and $E_{a,l}$ correspond to $E_h + E_-$ and $E_h + E_+$ in our model. Our $E_\pm$ is the *excess* energy, relative to the hopping barrier, required for adatom attachment/detachment.

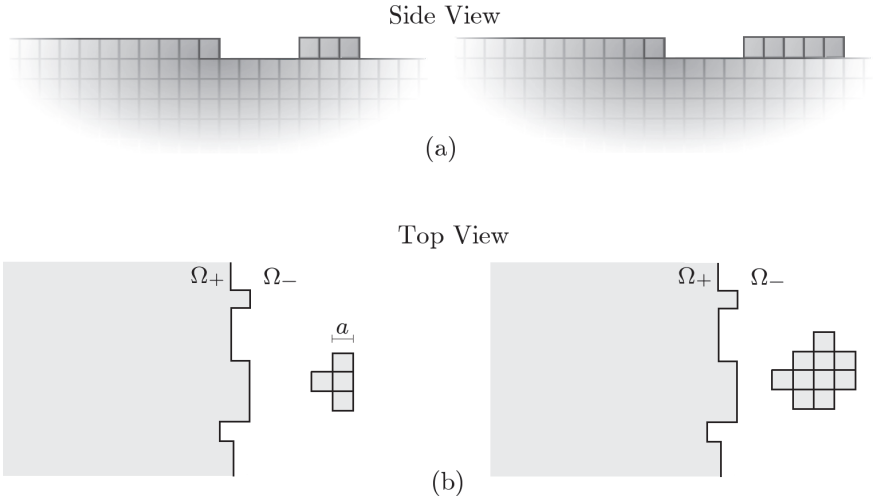

FIG. 13. *Islands in one dimension versus two dimensions. In this figure, we assume that adatoms interact (i.e., form bonds) with their nearest neighbors.* (a) *One dimension: all islands have one broken bond.* (b) *Two dimensions: smaller islands (left) have fewer broken bonds than larger islands (right). The symbol $\Omega_\pm$ denotes the upper (+) and lower (−) terraces. Since the energy cost to create an island increases with the number of broken bonds, larger islands are typically less probable than small islands.*

large N (recall $c^\pm \to c^{\rm eq}$ unless $\phi_\pm = \mathcal{O}(1/N)$), so that the step moves on a timescale of t/N.

7.4. Limitations of KMC model. Our KMC model has limitations due to the fact that we consider only a single step in one dimension. In this setting, it is not possible to derive step interactions. In many formulations of the BCF theory, such interactions introduce an additional energy into the step chemical potential, so that the energy cost of adatom detachment depends on the widths of the terraces adjacent to the step [18, 31, 32, 33]. Because the step chemical potential is equal to the edge atom bond energy in our derivation, we speculate that in an appropriate multistep KMC model, step interactions should appear as an additional contribution to E_b that depends on the distance between edge atoms.

Because our KMC model is only 1D, we cannot account for the effects of anisotropy in the crystal lattice. Such effects could be important in systems such as Si(001), where diffusion rates are both direction- and position-dependent [35, 36]. We speculate that an appropriate KMC model incorporating these features would lead to a BCF model with an anisotropic and (potentially) position-dependent diffusion coefficient.

Our analysis is also unable to determine the role that kinks play in the derivation of BCF-type models. In 2D KMC models, it is known that kinks, which alter the microscopic step profile, play an important role in determining the rates of adatom attachment/detachment processes. Moreover, in 2D BCF-type models, the chemical potential (i.e., the energy cost to remove an adatom from a step) and, consequently, the linear kinetic relations, are typically assumed to depend on the local step curvature [33]. However, a derivation that expresses this dependence remains an open question.

8. Conclusion. In this paper, we formally derived a BCF-type model, with correction terms, from a KMC master equation for a single step in one dimension. The

central ideas of our approach were to (i) connect the atomistic model to the BCF-type model via the notion of ensemble averages, and (ii) show that the BCF-type model describes a surface with few adatoms (i.e., a surface in a low-density regime). We also demonstrated that for systems close enough to equilibrium and at low enough temperatures, a low-density approximation applies for all times. Specifically, our analysis provided a definition of what constitutes near-equilibrium conditions (cf. Definitions 5.6 and 6.7) and showed that multi-adatom correlations, which contribute corrections to the BCF-type theory, are negligible under these conditions.

Our analysis (i) revealed the regions of parameter space in the KMC model that lead to diffusion limited kinetics and attachment/detachment limited kinetics in the BCF-type model, and (ii) indicated the atomistic origin (coming from the energy barriers of the KMC model) of the step chemical potential for the step continuum system.

In the context of our atomistic perspective, we believe that our averaging procedure implied by (6.2) is the first instance of an analytic definition of a step. This definition allowed us to derive a BCF-type model, specifically the step velocity law and linear kinetic relations at the step edge.

Our analysis leaves several open questions. Because our KMC model contains a single step, we are not able to account for step interactions. Moreover, the 1D nature of our analysis prohibits us from determining the roles that lattice anisotropy and kinks play in the derivation of BCF-type models. In particular, an important task is to derive the 2D step chemical potential, which is expected to depend on the step curvature. An additional challenge is to include external material deposition, which could increase the adatom correlations.

Appendix A. On solutions of 1-p and m-p models. In this appendix, we prove certain properties of the models introduced in section 4. First, we address the 1-p model.

LEMMA A.1. *In the* 1*-p model* (4.17)–(4.21)*, any state* j *can evolve to any other state* j' *in a finite number of transitions.*

Proof. By (4.24), there exists a finite sequence $\{T_{j\pm1,j}, T_{j\pm2,j\pm1}, \dots, T_{s_0,s_0\mp1}\}$ of transitions corresponding to the trajectory of states $\mathrm{j} \to \mathrm{j}\pm1 \to \mathrm{j}\pm2 \to \cdots \to s_0\mp1 \to s_0$, where the upper sign corresponds to the case $\mathrm{j} < s_0$ and the lower sign corresponds to $\mathrm{j} > s_0$. Moreover, the reverse rate for each of these processes is nonzero, so that there exists a sequence of transitions from s_0 to j. Hence, every j can access every j' in a finite number of transitions via the state s_0. ∎

In view of Lemma A.1, the matrix $\mathbf{T}$ is irreducible.

LEMMA A.2. *The* $\mathbf{T}$*-matrix described by* (4.24) *satisfies the Kolmogorov criterion. That is, for any closed loop of states* $j \to k \to l \to \cdots \to m \to j$*, the product of rates in the forward direction equals the product of rates in the backward direction; i.e., the transition rates satisfy* $T_{k,j}T_{l,k}\dots T_{j,m} = T_{m,j}\dots T_{k,l}T_{j,k}$ *(summation not implied).*

Proof. By (4.24), the transition rates satisfy $T_{j,j'} = T_{j',j}$ whenever $j, j' \neq s_0$. Thus, if the sequence of states does not contain s_0, the result is trivial. Next, assume that the sequence of states contains s_0, so that the transitions $s_0 \to s_0\pm1$, $s_0\pm1 \to s_0$ or $s_0 \to s_0 \pm 1$, $s_0 \mp 1 \to s_0$ will appear in the sequence of transitions. In these cases, the product of transition rates in the forward direction will include either the product $T_{s_0,s_0\pm1}T_{s_0\pm1,s_0} = D^2k\phi_\pm^2$ or the product $T_{s_0,s_0\pm1}T_{s_0\mp,s_0} = D^2k\phi_+\phi_-$. These products equal the products of transition rates in the reverse directions. Hence, the Kolmogorov criterion holds. ∎

Next, we show corresponding results for the m-p model.

LEMMA A.3. *In the m-p model* (4.2)–(4.10)*, any state* $\mathfrak{a}$ *can evolve to any other state* $\mathfrak{a}'$ *in a finite number of transitions.*

Proof. We proceed by induction. First, we prove that a 1-p state can transition to a 0-p state. Then, assuming that any m-particle can transition to an $(m-1)$-particle state, we show that any $(m+1)$-particle state can transition to an m-particle state.

Consider the case $\mathfrak{a} = \{j\}$. From (4.5) and (4.8), state $\mathfrak{a}$ can evolve into 0-p state $\mathfrak{a}' = \{\}$ via a finite sequence of transitions of the form $\{T_{\{j-1\},\{j\}}, T_{\{j-2\},\{j-1\}}, \dots, T_{\{s_0\},\{s_0+1\}}\}$.

Next, assume that all states $\mathfrak{a}$ for which $|\mathfrak{a}| \le m$ can evolve to an $(m-1)$-particle state via a finite sequence of transitions. We show that all $\mathfrak{a}'$ for which $|\mathfrak{a}'| = m+1$ can also evolve to an m-particle state via a finite sequence of transitions. If $\mathbb{1}_{\mathfrak{a}'}(s_0 - |\mathfrak{a}'| + 2) = n > 1$, then by (4.5) we choose a sequence of $n-1$ transitions in which an adatom moves to the right by one lattice site. We call this new state $\mathfrak{a}''$, for which $\mathbb{1}_{\mathfrak{a}'}(s_0 - |\mathfrak{a}''| + 2) = 1$. By (4.8), we add to this sequence a transition in which an adatom attaches to the step from the right, yielding a new state $\mathfrak{a}'''$. But $\mathfrak{a}'''$ has the property that $|\mathfrak{a}'''| = m$. This concludes the induction scheme.

Because all transitions are reversible, there exists a sequence of transitions from $\{\}$ to $\mathfrak{a}'$. Hence, any state $\mathfrak{a}$ can evolve to $\mathfrak{a}'$ by first transitioning to $\{\}$. ∎

In view of Lemma A.3, the T-matrix given by (4.2)–(4.10) is irreducible.

LEMMA A.4. *The T-matrix given by* (4.2)–(4.10) *satisfies the Kolmogorov criterion.*

Proof. All transitions $\mathfrak{a} \to \mathfrak{a}'$ for which $|\mathfrak{a}| = |\mathfrak{a}'|$ have the same transition rate. Therefore, the product of forward rates for any sequence of transitions $(\mathfrak{a} = \alpha) \to (\mathfrak{a}' = \boldsymbol{\alpha}') \to \cdots \to (\mathfrak{a}''' = \boldsymbol{\alpha}''') \to (\mathfrak{a} = \boldsymbol{\alpha})$ equals the product of the reverse rates. Moreover, in any closed loop of transitions, any transition $\mathfrak{a} \to \mathfrak{a}'$ for which $|\mathfrak{a}| = |\mathfrak{a}'| \pm 1$ introduces either the product $T_{\boldsymbol{\alpha},\boldsymbol{\alpha}\uplus\{s_0-|\boldsymbol{\alpha}|-1\pm1\}} T_{\boldsymbol{\alpha}\uplus\{s_0-|\boldsymbol{\alpha}|-1\pm1\},\boldsymbol{\alpha}} = D^2 k \phi_\pm^2$ or the product $T_{\boldsymbol{\alpha},\boldsymbol{\alpha}\uplus\{s_0-|\boldsymbol{\alpha}|-1\pm1\}} T_{\boldsymbol{\alpha}\uplus\{s_0-|\boldsymbol{\alpha}|-1\mp1\},\boldsymbol{\alpha}} = D^2 k \phi_+ \phi_-$ into the product of transition rates. These products equal the products of the corresponding transition rates in the reverse direction. ∎

The existence and uniqueness of solutions to the 1-p and m-p models are guaranteed by the following proposition.

PROPOSITION A.5. *If* $\mathbf{T}$ *is irreducible and satisfies the Kolmogorov criterion, then the system of ODEs* $\dot{p}_{\boldsymbol{\alpha}} = T_{\boldsymbol{\alpha},\boldsymbol{\alpha}'} p_{\boldsymbol{\alpha}'}$ *has a unique steady state solution when* $t \to \infty$.

For a proof of this proposition, see [49], for example.

Appendix B. Derivation of maximum principles for the 1-p and m-p models. We first consider a derivation of the maximum principle of Proposition 5.4 for the 1-p model.

PROPOSITION B.1. *Let* $p_j(t)$ *be the solution to* (4.17)–(4.21) *with initial data* $p_j(0)$*, and define* $\hat{p}_j = p_j/k$ *for* $j \neq s_0$ *and* $\hat{p}_{s_0} = p_{s_0}$*. Then* $\hat{p}_j$ *satisfies the maximum principle that* $\max_j\{\hat{p}_j(t)\} \le \max_j\{\hat{p}_j(0)\}$ *for all* $t > 0$.

Proof. We proceed by reductio ad absurdum. Writing (4.17)–(4.21) in terms of $\hat{p}_j$ yields

$$
\begin{aligned}
k\dot{\hat{p}}_j &= Dk[\hat{p}_{j+1} - 2\hat{p}_j + \hat{p}_{j-1}], \qquad j \neq s_0, s_0 \pm 1,\\
k\dot{\hat{p}}_{s_0\pm1} &= Dk[\phi_\pm \hat{p}_{s_0} - (1+\phi_\pm)\hat{p}_{s_0\pm1} + \hat{p}_{s_0\pm2}],\\
\dot{\hat{p}}_{s_0} &= Dk[\phi_- \hat{p}_{s_0-1} - (\phi_- + \phi_+)\hat{p}_{s_0} + \phi_+ \hat{p}_{s_0+1}].
\end{aligned} \tag{B.1}
$$

Let us assume that at some time t there is an l such that $\dot{\hat{p}}_l(t) \geq 0$ and $\hat{p}_l(t) \geq \hat{p}_j(t)$ for all $j \neq l$. By virtue of (B.1), we infer that

$$\hat{p}_l(t) \geq \frac{\theta_1 \hat{p}_{l-1}(t) + \theta_2 \hat{p}_{l+1}(t)}{\theta_1 + \theta_2},$$

where $\theta_{1,2}$ stand for 1 or $\phi_\pm$, depending on the value of l. By assumption, it is impossible to have $\hat{p}_{l\pm1}(t) > \hat{p}_l(t)$, so that either $\hat{p}_l$ is not a maximum or $\hat{p}_j$ is constant for all j. ∎

Next we derive the maximum principle of Proposition 6.5 for the m-p model.

PROPOSITION B.2. *Assume that $p_{\boldsymbol{\alpha}}(t)$ is the solution to $\dot{p}_{\boldsymbol{\alpha}}(t) = T_{\boldsymbol{\alpha},\boldsymbol{\alpha}'} p_{\boldsymbol{\alpha}'}(t)$, where $T_{\boldsymbol{\alpha},\boldsymbol{\alpha}'}$ is given by* (4.2)–(4.10) *(summation is implied over repeated multisets). Moreover, assume that $|\boldsymbol{\alpha}| \leq m$ for all $\boldsymbol{\alpha}$, where m is some positive integer, and define $\hat{p}_{\boldsymbol{\alpha}}(t) := p_{\boldsymbol{\alpha}}(t)/k^{|\boldsymbol{\alpha}|}$. Then $\hat{p}_{\boldsymbol{\alpha}}(t)$ satisfies the maximum principle that $\max_{\boldsymbol{\alpha}}\{\hat{p}_{\boldsymbol{\alpha}}(t)\} \leq \max_{\boldsymbol{\alpha}}\{\hat{p}_{\boldsymbol{\alpha}}(0)\}$ for all times $t > 0$.*

Proof. We proceed by reductio ad absurdum. Written in terms of the rescaled probabilities $\hat{p}_{\boldsymbol{\alpha}}$, (4.1) becomes

$$k^{|\boldsymbol{\alpha}|} \frac{d\hat{p}_{\boldsymbol{\alpha}}}{dt} = \sum_{\boldsymbol{\alpha}'} T_{\boldsymbol{\alpha},\boldsymbol{\alpha}'} k^{|\boldsymbol{\alpha}'|} \hat{p}_{\boldsymbol{\alpha}'}(t) \tag{B.2}$$

(we now write summations explicitly to avoid confusion). Suppose that there is a maximum $\hat{p}_{\boldsymbol{\alpha}}(t)$ at some time t, i.e., $\hat{p}_{\boldsymbol{\alpha}}(t) \geq \hat{p}_{\boldsymbol{\alpha}'}(t)$ for all $\boldsymbol{\alpha}' \neq \boldsymbol{\alpha}$ and $d\hat{p}_{\boldsymbol{\alpha}}/dt \geq 0$. Recalling (4.10), we conclude that

$$\sum_{\substack{\boldsymbol{\alpha}' \\ \boldsymbol{\alpha}' \neq \boldsymbol{\alpha}}} T_{\boldsymbol{\alpha},\boldsymbol{\alpha}'} \mathfrak{b}_{\boldsymbol{\alpha}'} k^{|\boldsymbol{\alpha}'|} \geq k^{|\boldsymbol{\alpha}|} \sum_{\substack{\boldsymbol{\alpha}' \\ \boldsymbol{\alpha}' \neq \boldsymbol{\alpha}}} T_{\boldsymbol{\alpha}',\boldsymbol{\alpha}}, \tag{B.3}$$

where $\mathfrak{b}_{\boldsymbol{\alpha}'} := \hat{p}_{\boldsymbol{\alpha}'}/\hat{p}_{\boldsymbol{\alpha}} \leq 1$ by assumption. We now compare elements of each sum term by term in (B.3). In view of (4.2)–(4.10), we consider the following three possible cases (summation is not implied over repeated indices):

(i) if $|\boldsymbol{\alpha}| = |\boldsymbol{\alpha}'|$, then $T_{\boldsymbol{\alpha},\boldsymbol{\alpha}'} = T_{\boldsymbol{\alpha}',\boldsymbol{\alpha}}$;

(ii) if $|\boldsymbol{\alpha}| = |\boldsymbol{\alpha}'| + 1$, then $T_{\boldsymbol{\alpha},\boldsymbol{\alpha}'} k^{|\boldsymbol{\alpha}'|} = T_{\boldsymbol{\alpha}',\boldsymbol{\alpha}} k^{|\boldsymbol{\alpha}|}$; and

(iii) if $|\boldsymbol{\alpha}| = |\boldsymbol{\alpha}'| - 1$, then $T_{\boldsymbol{\alpha},\boldsymbol{\alpha}'} k^{|\boldsymbol{\alpha}'|} = T_{\boldsymbol{\alpha}',\boldsymbol{\alpha}} k^{|\boldsymbol{\alpha}|}$.

Comparing the right- and left-hand sides of (B.3), we therefore see that the inequality holds only when $\mathfrak{b}_{\boldsymbol{\alpha}'} = 1$ for every $\boldsymbol{\alpha}'$, which concludes the proof. ∎

Acknowledgments. We wish to thank T. L. Einstein, J. W. Evans, G. M. Gallatin, J. Krug, G. McFadden, T. P. Schultz, P. Smereka, and J. Weare for helpful discussions during the preparation of this paper. We are also grateful for the hospitality extended to us by the Institute for Pure and Applied Mathematics (IPAM) at the University of California, Los Angeles, in the fall of 2012, when part of this work was completed.

REFERENCES

[1] D. M. ACKERMAN AND J. W. EVANS, *Boundary conditions for Burton–Cabrera–Frank type step-flow models: Coarse-graining of discrete 2D deposition-diffusion equations*, Multiscale Model. Simul., 9 (2011), pp. 59–88.

[2] J. G. AMAR, *The Monte Carlo method in science and engineering*, Comput. Sci. Eng., 8 (2006), pp. 9–19.

[3] J. G. Amar and F. Family, *Critical cluster size: Island morphology and size distribution in submonolayer epitaxial growth*, Phys. Rev. Lett., 74 (1995), pp. 2066–2069.
[4] A. B. Bortz, M. H. Kalos, and J. L. Lebowitz, *A new algorithm for Monte Carlo simulation of Ising spin systems*, J. Comput. Phys., 17 (1975), pp. 10–18.
[5] W. K. Burton, N. Cabrera, and F. C. Frank, *The growth of crystals and the equilibrium structure of their surfaces*, Philos. Trans. R. Soc. London Ser. A, 243 (1951), pp. 299–358.
[6] A. Chatterjee and D. G. Vlachos, *An overview of spatial microscopic and accelerated kinetic Monte Carlo methods*, J. Comput.-Aided Mater. Des., 14 (2007), pp. 253–308.
[7] T. Chou, K. Mallick, and R. K. P. Zia, *Non-equilibrium statistical mechanics: From a paradigmatic model to biological transport*, Rep. Prog. Phys., 74 (2011), 116601.
[8] W. E and N. K. Yip, *Continuum theory of epitaxial crystal growth.* I, J. Stat. Phys., 104 (2001), pp. 221–253.
[9] G. Ehrlich and F. G. Hudda, *Atomic view of surface self-diffusion: Tungsten on Tungsten*, J. Chem. Phys., 44 (1966), pp. 1039–1049.
[10] P. Gambardella, H. Brune, K. Kern, and V. I. Marchenko, *Equilibrium island-size distribution in one dimension*, Phys. Rev. B, 73 (2006), 245425.
[11] R. Ghez, H. G. Cohen, and J. B. Keller, *The stability of growing or evaporating crystals*, J. Appl. Phys., 73 (1993), pp. 3685–3693.
[12] R. Ghez and S. S. Iyer, *The kinetics of fast steps on crystal surfaces and its application to the molecular beam epitaxy of silicon*, IBM J. Res. Dev., 32 (1988), pp. 804–818.
[13] D. T. Gillespie, *A general method for numerically simulating the stochastic time evolution of coupled chemical reactions*, J. Comput. Phys., 22 (1976), pp. 403–434.
[14] A. B. H. Hamouda, A. Pimpinelli, and T. L. Einstein, *Relaxation of terrace-width distributions: Physical information from Fokker-Planck time*, Surf. Sci., 602 (2008), pp. 3569–3577.
[15] P. Hänggi, P. Talkner, and M. Borkovec, *Reaction-rate theory: Fifty years after Kramers*, Rev. Modern Phys., 62 (1990), pp. 251–341.
[16] N. Israeli and D. Kandel, *Profile of a decaying crystalline cone*, Phys. Rev. B, 60 (1999), pp. 5946–5962.
[17] N. Israeli and D. Kandel, *Decay of one-dimensional surface modulations*, Phys. Rev. B, 62 (2000), pp. 13707–13717.
[18] H.-C. Jeong and E. D. Williams, *Steps on surfaces: Experiment and theory*, Surf. Sci. Rep., 34 (1999), pp. 171–294.
[19] F. P. Kelly, *Reversibility and Stochastic Networks*, Wiley, New York, 1979.
[20] S. Kodiyalam, K. E. Khor, and S. Das Sarma, *Calculated Schwoebel barriers on Si*(111) *steps using an empirical potential*, Phys. Rev. B, 53 (1996), pp. 9913–9922.
[21] R. V. Kohn, T. S. Lo, and N. K. Yip, *Continuum limit of a step flow model of epitaxial growth*, in Statistical Mechanical Modeling in Materials Research, Mat. Res. Soc. Symp. Proc. 701, M. C. Bartelt, J. W. Evans, A. S. Karma, S. Torquato, and D. E. Wolf, eds., Materials Research Society, Warrendale, PA, 2002, pp. T1.7.1–T1.7.7.
[22] A. Kolmogorov, *Zur Theorie der Markoffschen Ketten*, Math. Ann., 112 (1936), pp. 155–160.
[23] K. A. Fichthorn and W. H. Weinberg, *Theoretical foundations of dynamical Monte Carlo simulations*, J. Chem. Phys., 95 (1991), pp. 1090–1096.
[24] M. D. Johnson, K. T. Leung, A. Birch, B. G. Orr, and J. Tersoff, *Adatom concentration on GaAs*(001) *during MBE annealing*, Surf. Sci., 350 (1996), pp. 254–258.
[25] F. Liu and H. Metiu, *Stability and kinetics of step motion on crystal surfaces*, Phys. Rev. E, 49 (1994), pp. 2601–2616.
[26] C. N. Luse, A. Zangwill, D. D. Vvedensky, and M. R. Wilby, *Adatom mobility on vicinal surfaces during epitaxial growth*, Surf. Sci., 274 (1992), pp. L535–L540.
[27] D. Margetis, P. N. Patrone, and T. L. Einstein, *Stochastic models of epitaxial growth*, in Advances in Spectroscopy and Imaging of Surfaces and Nanostructures, Mater. Res. Soc. Proc. 1318, Materials Research Society, Warrendale, PA, 2011, pp. 1–6.
[28] C. Misbah, O. Pierre-Louis, and Y. Saito, *Crystal surfaces in and out of equilibrium: A modern view*, Rev. Modern Phys., 82 (2010), pp. 981–1040.
[29] R. K. Pathria, *Statistical Mechanics*, 2nd ed., Butterworth-Heinemann, Woburn, MA, 1996.
[30] P. N. Patrone, R. E. Caflisch, and D. Margetis, *Characterizing equilibrium in epitaxial growth*, Europhys. Lett., 97 (2012), 48012.
[31] P. N. Patrone, T. L. Einstein, and D. Margetis, *One-dimensional model of interacting-step fluctuations on vicinal surfaces: Analytical formulas and kinetic Monte Carlo simulations*, Phys. Rev. E, 82 (2010), 061601.
[32] P. N. Patrone, R. Wang, and D. Margetis, *Small fluctuations in epitaxial growth via conservative noise*, J. Phys. A, 44 (2011), 31.
[33] O. Pierre-Louis and C. Misbah, *Dynamics and fluctuations during MBE on vicinal surfaces.* I. *Formalism and results of linear theory*, Phys. Rev. B, 58 (1998), pp. 2259–2275.

[34] O. Pierre-Louis and C. Misbah, *Dynamics and fluctuations during MBE on vicinal surfaces. II. Nonlinear analysis*, Phys. Rev. B, 58 (1998), pp. 2276–2288.
[35] C. Roland and G. H. Gilmer, *Epitaxy on surfaces vicinal to Si*(001). I. *Diffusion of silicon adatoms over the terraces*, Phys. Rev. B, 46 (1992), pp. 13428–13436.
[36] C. Roland and G. H. Gilmer, *Epitaxy on surfaces vicinal to Si*(001). II. *Growth properties of Si*(001) *steps*, Phys. Rev. B, 46 (1992), pp. 13437–13451.
[37] L. I. Rubinstein, *The Stefan Problem*, American Mathematical Society, Providence, RI, 1971.
[38] M. Saum and T. P. Schulze, *The role of processing speed in determining step patterns during directional epitaxy*, Discrete Contin. Dyn. Syst. Ser. B, 11 (2009), pp. 443–457.
[39] T. P. Schulze, *Morphological instability during directional epitaxy*, J. Cryst. Growth, 295 (2006), pp. 188–201.
[40] R. L. Schwoebel and E. J. Shipsey, *Step motion on crystal surfaces*, J. Appl. Phys., 37 (1966), pp. 3682–3686.
[41] W. Silvestri, A. P. Graham, and J. P. Toennies, *Adatom formation on the Ni*(110) *surface*, Phys. Rev. Lett., 81 (1998), pp. 1034–1037.
[42] T. Shitara, T. Suzuki, D. D. Vvedensky, and T. Nishinaga, *Concentration profiles of surface atoms during epitaxial growth on vicinal surfaces*, Appl. Phys. Lett., 62 (1993), pp. 1347–1349.
[43] S. Stoyanov, *Heating current induced conversion between* 2×1 *and* 1×2 *domains at vicinal* (001) *Si surfaces—can it be explained by electromigration of Si adatoms?*, Jpn. J. Appl. Phys., 29 (1990), pp. L659–L662.
[44] S. Stoyanov, *Electromigration induced step bunching on Si surfaces—how does it depend on the temperature and heating current direction?*, Jpn. J. Appl. Phys., 30 (1991), pp. 1–6.
[45] S. Stoyanov, *Current-induced step bunching at vicinal surfaces during crystal sublimation*, Surf. Sci., 370 (1997), pp. 345–354.
[46] S. Stoyanov, *New type of step bunching instability at vicinal surfaces in crystal evaporation affected by electromigration*, Surf. Sci., 416 (1998), pp. 200–213.
[47] J. Tersoff, M. D. Johnson, and B. G. Orr, *Adatom densities on GaAs: Evidence for near-equilibrium growth*, Phys. Rev. Lett., 78 (1997), pp. 282–285.
[48] J. P. van der Eerden, P. Bennema, and T. A. Cherepanova, *Survey of Monte Carlo simulations of crystal surfaces and crystal growth*, Prog. Cryst. Growth Ch., 1 (1978), pp. 219–254.
[49] N. G. Van Kampen, *Stochastic Processes in Physics and Chemistry*, 3rd ed., North–Holland, Amsterdam, 2007.
[50] A. F. Voter, *Introduction to the kinetic Monte Carlo method*, in Radiation Effects in Solids, NATO Sci. Ser. 235, K. E. Sickafus, E. A. Kotomin, and B. P. Uberuaga, eds., Springer, The Netherlands, 2007, pp. 1–23.
[51] J. D. Weeks and G. H. Gilmer, *Dynamics of crystal growth*, Adv. Chem. Phys., 40 (1979), pp. 157–228.
[52] W. M. Young and E. W. Elcock, *Monte Carlo studies of vacancy migration in binary ordered alloys:* I, Proc. Phys. Soc., 89 (1966), pp. 735–746.
[53] A. Zangwill, C. N. Luse, D. D. Vvedensky, and M. R. Wilby, *Equations of motion for epitaxial growth*, Surf. Sci., 274 (1992), pp. L529–L534.
[54] X. D. Zhu, *Determination of surface-diffusion kinetics of adatoms in epitaxy under step-flow growth conditions*, Phys. Rev. B, 57 (1998), pp. R9478–R9481.